Nonlinear electrochemical relaxation around conductors

Kevin T. Chu[1,2] and Martin Z. Bazant[1]
[1]*Department of Mathematics, Massachusetts Institute of Technology, Cambridge, Massachusetts 02139, USA*
[2]*Department of Mechanical and Aerospace Engineering, Princeton University, Princeton, New Jersey 08544, USA*
(Received 8 March 2006; published 6 July 2006)

We analyze the simplest problem of electrochemical relaxation in more than one dimension—the response of an uncharged, ideally polarizable metallic sphere (or cylinder) in a symmetric, binary electrolyte to a uniform electric field. In order to go beyond the circuit approximation for thin double layers, our analysis is based on the Poisson-Nernst-Planck (PNP) equations of dilute solution theory. Unlike most previous studies, however, we focus on the nonlinear regime, where the applied voltage across the conductor is larger than the thermal voltage. In such strong electric fields, the classical model predicts that the double layer adsorbs enough ions to produce bulk concentration gradients and surface conduction. Our analysis begins with a general derivation of surface conservation laws in the thin double-layer limit, which provide effective boundary conditions on the quasineutral bulk. We solve the resulting nonlinear partial differential equations numerically for strong fields and also perform a time-dependent asymptotic analysis for weaker fields, where bulk diffusion and surface conduction arise as first-order corrections. We also derive various dimensionless parameters comparing surface to bulk transport processes, which generalize the Bikerman-Dukhin number. Our results have basic relevance for double-layer charging dynamics and nonlinear electrokinetics in the ubiquitous PNP approximation.

DOI: 10.1103/PhysRevE.74.011501 PACS number(s): 82.45.Gj, 82.45.Jn, 66.10.−x

I. INTRODUCTION

Diffuse-charge dynamics plays an important role in the response of electrochemical and biological systems subject to time-dependent voltages or electric fields [1]. The classical example is impedance spectroscopy in electrochemistry [2–5], but electrochemical relaxation is also being increasingly exploited in colloids and microfluidics [6]. For example, alternating electric fields have been used to pump or mix liquid electrolytes [7–18], to separate or self-assemble colloids near electrodes [19–25], and to manipulate polarizable particles [16,26–31] or biological cells and vesicles [32–34].

In this paper, we analyze some simple problems exemplifying the nonlinear response of an electrolyte around an ideally polarizable object due to diffusion and electromigration. As shown in Fig. 1, we consider the ionic relaxation around a metallic sphere [Fig. 1(a)] or cylinder [Fig. 1(b)] subject to a suddenly applied uniform background electric field, as in metallic colloids. Equivalently, we consider a metallic hemisphere [Fig. 1(c)] or half cylinder [Fig. 1(d)] on an insulating plane, to understand relaxation around metallic structures on channel walls in microelectrochemical devices. Although we do not consider fluid flow, our analysis of nonlinear electrochemical relaxation is a necessary first step toward understanding associated problems of induced charge electro-osmosis in the same geometries [16–18,29–31], and thus it also has relevance for the case of ac electro-osmosis at planar electrode arrays [7–14].

In electrochemistry [35–38] and colloid science [39,40], it is common to assume that the charged double layer at a metal surface is very thin and thus remains in quasiequilibrium, even during charging dynamics. As a result, for over a century [1], the standard model of electrochemical relaxation has been an equivalent circuit, where the neutral bulk is represented by an Ohmic resistor and the double layer by a surface impedance [2–5], which reduces to a linear capacitor at an ideally polarizable surface. For our model problems, this "*RC* circuit" model was first applied to electrochemical relaxation around a sphere by Simonov and Shilov [41] and around a cylinder by Bazant and Squires [16,17]. Similar *RC*-circuit analysis has been applied extensively to planar electrode arrays in microfluidic devices, following Ramos *et al.* [7] and Ajdari [8].

While convenient for mathematical analysis and often sufficiently accurate, circuit models neglect the possibility of bulk concentration gradients, which can arise at large applied voltages [1] and/or when the surface is highly charged [42–45], as well as nonuniform surface transport of ions through the double layer [46,47]. Dukhin and Shilov [42,45] and later Hinch and co-workers [43,44] made significant progress beyond the simple circuit model by including bulk

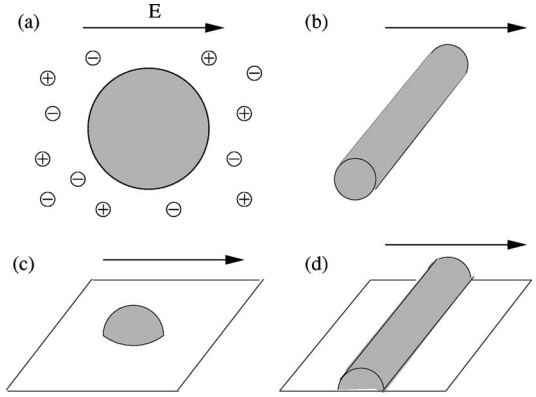

FIG. 1. (a) Schematic diagram of metallic colloidal sphere in a binary electrolyte subjected to an applied electric field, which has the same relaxation as a metallic hemisphere on a flat insulting surface, shown in (c). We also consider the analogous two-dimensional problems of a metallic cylinder (b) or a half cylinder on an insulating plane (d).

diffusion in their studies of double-layer polarization around highly charged spherical particles (of fixed charged density) in weak applied fields. One of the main results of their analysis is that for weak applied electric fields, bulk concentration gradients appear as a small correction (on the order of the applied electric field) to a uniform background concentration. In this work, we will lift the weak-field restriction and consider the nonlinear response of the system to strong applied fields, using the same mathematical model as in all prior work—the Poisson-Nernst-Planck (PNP) equations of dilute solution theory [38]. As we shall see, nonlinear response generally involves non-negligible bulk diffusion.

There are also difficulties with the traditional macroscopic picture of the double layer as an infinitely thin surface impedance, or possibly some more general nonlinear circuit element. At the microscopic level, the double layer has a more complicated structure with at least two different regimes: a diffuse layer where the ions move freely in solution and a compact surface layer, where ions may be condensed in a Stern monolayer with its own physical features (such as surface capacitance, surface diffusivity, and surface roughness) [35–37]. The surface capacitance may also include the effect of a dielectric coating, where ions do not penetrate [8]. Mathematically, in one dimension the capacitor model can be derived as an effective boundary condition for the neutral bulk (Nernst-Planck) equations by asymptotic analysis of the PNP equations in the thin double-layer limit [1]. Extending this analysis to higher dimensions, however, requires allowing for tangential "surface conduction" through the double layer on the conductor for large applied electric fields. Here, we derive effective boundary conditions for the neutral bulk in the PNP model by following a general mathematical method for surface conservation laws at microscopically diffuse interfaces [48].

The nonlinear response of electrochemical systems to strong applied fields seems to be relatively unexplored. To our knowledge, the only prior mathematical study of nonlinear relaxation with the PNP model is the recent work of Bazant, Thornton, and Ajdari on the one-dimensional problem of parallel-plate blocking electrodes applying a sudden pulsed voltage [1]. (The same analysis has been recently extended to "modified PNP" models accounting for steric effects in concentrated solutions [49], which would also be an important extension of our work.) For applied voltages in the *weakly nonlinear* regime, which is analogous to weak applied fields in our problems, they find that the relaxation of the cell to the steady state requires bulk diffusion processes that appear as a small correction at $O(\epsilon)$, where the small parameter ϵ is the ratio of the Debye length to a typical scale of the geometry. (In contrast, in Refs. [42–45], it appears that primarily the strength of the applied electric field is assumed to be small, although the mathematical limit is not explicitly defined.) For applied voltages in the *strongly nonlinear* regime, they show that bulk concentration gradients can no longer be considered small, since $O(1)$ concentration variations appear. In both regimes, the absorption of neutral salt by the double layer (and therefore the buildup of surface ion density) is the key driving force for bulk diffusion. This positive salt adsorption in response to an applied voltage, first noted in Ref. [1], is opposite to the classical "Donnan effect" of salt expulsion [40], which occurs if the surface chemically injects or removes ions during the initial creation of the double layer [50].

Bazant *et al.* also emphasize the importance of both the charging and the diffusion time scales in the evolution of electrochemical systems [1]. Because circuit models inherently neglect diffusion processes, the only characteristic dynamic time scale that appears is the so-called *RC* charging time $\tau_c=\lambda_D L/D$, where λ_D is the Debye length, L is the system size, and D is the characteristic diffusivity of the ions.[1] However, when concentration gradients are present, diffusion processes and dynamics at the diffusion time scale $\tau_L=L^2/D$ may be important. Most theoretical analyses of electrochemical systems only consider the dynamics at one of these two dominant time scales—effectively decoupling the dynamics at the two time scales. This decoupling of the dynamics is natural when one considers the wide separation in the time scales that govern the evolution of the system: $\tau_L \gg \tau_c$. An interesting discussion of how the two time scales are coupled using ideas related to time-dependent asymptotic matching is presented in Ref. [1].

The paper is organized as follows. We begin in Sec. II by carefully considering the thin double-layer limit of our model problems, which leads to effective boundary conditions for the neutral bulk equations in Sec. III. The most interesting boundary conditions developed are surface conservation laws, whose physical content we discuss in detail in Sec. IV, where we also define dimensionless parameters governing the importance of various surface transport processes. In Sec. V, we explore the steady response to large applied electric fields in our model problems; a notable prediction is the formation of recirculating bulk diffusion currents coupled to surface transport processes. We then turn to relaxation dynamics in the three regimes identified by Bazant *et al.* [1], using similar methods, albeit with nontrivial modifications for two or three dimensions. We begin with the linear response to a weak field in Sec. VI, where we obtain exact solutions using transform methods for arbitrary double-layer thickness and also consider ac electric fields. Next, in Sec. VII we use boundary-layer methods in space and time to analyze weakly nonlinear relaxation in somewhat larger fields, in the asymptotic limit of thin double layers. Finally, in Sec. VIII we comment on the challenges of strongly nonlinear relaxation, where bulk diffusion and surface conduction dominate the dynamics. We conclude in Sec. IX by discussing limitations of the PNP model and directions for future research.

[1]Note that when charging is driven by an externally applied voltage or field, the relevant relaxation time for double-layer charging is not the often quoted Debye time $\tau_D=\lambda_D^2/D$ [39,51]. The Debye time is the correct characteristic response time for double-layer charging only in the unphysical scenario where charge is instantaneously placed on the particle (as opposed to transported through the electrolyte) [52]. This result has been discovered many times by different scientific communities [1,53–56] but only recently seems to be gaining widespread understanding.

II. MATHEMATICAL MODEL

A. PNP initial-boundary-value problem

As a model problem, we consider the response of an isolated, ideally polarizable sphere (or cylinder) subjected to a uniform, applied electric field, as shown in Fig. 1. For simplicity, we focus only on a symmetric, binary electrolyte where both ionic species have the same diffusivity and charge number. In order to study nonlinear effects and avoid imposing a time scale, we assume that the uniform electric field is suddenly applied at $t=0$.

As in most (if not all) prior work on electrochemical dynamics, we assume the Poisson-Nernst-Planck equations of dilute solution theory [38],

$$\frac{\partial C_+}{\partial t} = \nabla \cdot \left(D\nabla C_+ + \frac{z_+ eD}{kT} C_+ \nabla \Phi \right), \tag{1}$$

$$\frac{\partial C_-}{\partial t} = \nabla \cdot \left(D\nabla C_- - \frac{z_+ eD}{kT} C_- \nabla \Phi \right), \tag{2}$$

$$-\varepsilon_s \nabla^2 \Phi = z_+ e(C_+ - C_-), \tag{3}$$

where D is the diffusivity, z_+ is the charge number of the positively charged species, e is the charge of a proton, k is Boltzmann's constant, T is the absolute temperature, and ε_s is the electric permittivity of the solution. As usual, we have used the Nernst-Einstein relation to write the mobility in terms of the diffusivity $b=D/kT$. It is also useful to define the chemical potentials of the ions,

$$\mu_\pm = kT \ln C_\pm \pm z_+ e\Phi \tag{4}$$

from which their fluxes are defined as $\mathbf{F}_\pm = -bC_\pm \nabla \mu_\pm$.

At the conductor's surface, we assume the same boundary conditions as in Ref. [1]. We adopt a linear surface capacitance condition on the electrostatic potential [57],

$$\Phi + \lambda_S \frac{\partial \Phi}{\partial n} = V, \tag{5}$$

where λ_S is a length characterizing the compact-layer surface capacitance (e.g., due to a Stern monolayer or a thin dielectric coating), where V is the potential of the conductor, which is set either externally or by the condition of fixed total charge [16,17,28]. (We will focus on the case of zero total charge, where symmetry implies $V=0$ in our simple geometries.) To focus on charging dynamics, we also assume an ideally polarizable surface with no-flux boundary conditions:

$$D\frac{\partial C_+}{\partial n} + \frac{z_+ eD}{kT} C_+ \frac{\partial \Phi}{\partial n} = 0, \tag{6}$$

$$D\frac{\partial C_-}{\partial n} - \frac{z_+ eD}{kT} C_- \frac{\partial \Phi}{\partial n} = 0, \tag{7}$$

where the direction of the unit normal is taken to point inward towards the center of the sphere (i.e., *outward* from the region occupied by the electrolyte solution). In the far field, we assume that both the concentration and potential profiles tend toward their initial conditions, given everywhere by

TABLE I. Summary of notations for the various ion fluxes and chemical potentials, before and after scaling.

	Dimensional formula[a]	Dimensionless formula
$\mu_\pm$	$kT \ln C_\pm \pm z_+ e\Phi$	$\ln c_\pm \pm \phi$
$\mathbf{F}_\pm$	$-bC_\pm \nabla \mu_\pm$	$-c_\pm \nabla \mu_\pm$
	$-\left(D\nabla C_\pm \pm \frac{z_+ eD}{kT} C_\pm \nabla \Phi\right)$	$-(\nabla c_\pm \pm c_\pm \nabla \phi)$
$\mathbf{F}_\pm^{(d)}$	$-D\nabla C_\pm$	$-\nabla c_\pm$
$\mathbf{F}_\pm^{(e)}$	$\mp \frac{z_+ eD}{kT} C_\pm \nabla \Phi$	$\mp c_\pm \nabla \phi$
$\mathbf{F}_c$	$-\left(D\nabla C + \frac{z_+ eD}{kT} \rho \nabla \Phi\right)$	$-(\nabla c + \rho \nabla \phi)$
$\mathbf{F}_c^{(d)}$	$-D\nabla C$	$-\nabla c$
$\mathbf{F}_c^{(e)}$	$-\frac{z_+ eD}{kT} \rho \nabla \Phi$	$-\rho \nabla \phi$
$\mathbf{F}_\rho$	$-\left(D\nabla \rho + \frac{z_+ eD}{kT} C \nabla \Phi\right)$	$-(\nabla \rho + c \nabla \phi)$
$\mathbf{F}_\rho^{(d)}$	$-D\nabla \rho$	$-\nabla \rho$
$\mathbf{F}_\rho^{(e)}$	$-\frac{z_+ eD}{kT} C \nabla \Phi$	$-c \nabla \phi$

[a]In these formulas, ρ is half the charge density (not the total charge density). Also, we have abused notation and used the same variable ρ for both the dimensional and dimensionless formulas. ρ in the dimensional formulas is equal to $C_0\rho$ in the dimensionless formulas.

$$C_\pm(R, \theta, \phi, t=0) = C_0, \tag{8}$$

$$\Phi(R, \theta, \phi, t=0) = -E_0 R\left(1 - \frac{a^3}{R^3}\right)\cos\theta, \tag{9}$$

where a is the radius of the sphere, C_0 is the bulk concentration far away from the conductor, and E_0 is the applied electric field. For the case of the cylinder, the initial conditions for the concentration profile remain the same and the initial electric potential takes the form

$$\Phi(R, \theta, t=0) = -E_0 R\left(1 - \frac{a^2}{R^2}\right)\cos\theta. \tag{10}$$

B. Different contributions to ion transport

The transport equations (1) and (2) represent conservation laws for the ionic species where the flux of each species is a combination of diffusion and electromigration. Because this paper examines ionic fluxes in detail, let us take a moment to fix the notation that we shall use to discuss different contributions to charge and mass transport. All fluxes will be denoted by the variable $\mathbf{F}$ (or F for scalar components of flux). Superscripts will be used to distinguish between the diffusion (d) and electromigration (e) contributions to the flux. Subscripts will be used to denote the species or quantity with which the flux is associated. Finally, normal and tangential components of a flux will be denoted through the use of an extra subscript: n for the normal component and t for the tangential component. As examples, $\mathbf{F}_+^{(e)} = -\frac{z_+ eD}{kT} C_+ \nabla \Phi$ represents the flux of the positively charged species due to electromigration and $F_{n,c}^{(d)} = -D\frac{\partial C}{\partial n}$ represents the flux of the neutral salt concentration $C=(C_+ + C_-)/2$ normal to a surface arising from diffusion. Table I provides a summary of the

various bulk fluxes that will arise in our discussion. (We also abuse notation and use the same symbol μ for a chemical potential with dimensions and scaled to kT.)

C. Dimensionless formulation

To facilitate the analysis of the model problem, it is convenient to nondimensionalize the governing equations and boundary conditions. Scaling the length by the radius of the sphere, a, the time by the diffusion time $\tau_D=a^2/D$, and the electric potential by the thermal voltage divided by the cation charge number, kT/z_+e, the governing equations (1)–(3) become

$$\frac{\partial c_+}{\partial t} = \nabla \cdot (\nabla c_+ + c_+ \nabla \phi), \tag{11}$$

$$\frac{\partial c_-}{\partial t} = \nabla \cdot (\nabla c_- - c_- \nabla \phi), \tag{12}$$

$$-\epsilon^2 \nabla^2 \phi = (c_+ - c_-)/2, \tag{13}$$

where $c_\pm$, ϕ, and t are the dimensionless concentrations, electric potential, and time, respectively, the spatial derivatives are with respect to the dimensionless position, and ϵ is the ratio of the Debye screening length $\lambda_D=\sqrt{\frac{\varepsilon_s kT}{2z_+^2 e^2 C_0}}$ to the radius of the sphere. The boundary conditions at the surface of the sphere and the initial conditions become

$$\phi + \delta\epsilon \frac{\partial \phi}{\partial n} = v, \tag{14}$$

$$\frac{\partial c_+}{\partial n} + c_+ \frac{\partial \phi}{\partial n} = 0, \tag{15}$$

$$\frac{\partial c_-}{\partial n} - c_- \frac{\partial \phi}{\partial n} = 0, \tag{16}$$

$$c_\pm(r,\theta,\phi,t=0) = 1, \tag{17}$$

$$\phi(r,\theta,\phi,t=0) = -E_0 r\left(1 - \frac{1}{r^3}\right)\cos\theta. \tag{18}$$

In the far field, the dimensionless concentrations approach 1 and the electric potential approaches $-E_0 r \cos\theta$. Note that in nondimensionalizing the surface capacitance boundary condition (5), we have chosen to introduce a new dimensionless parameter $\delta \equiv \lambda_S/\lambda_D$ which makes it possible to study the effects of the Stern layer capacitance independently from the double-layer thickness [57].

Because the charge density and neutral salt concentration are important for understanding the behavior of electrochemical transport at high applied fields, it is often useful to formulate the governing equations in terms of the average concentration $c=(c_+ + c_-)/2$ and half the charge density $\rho = (c_+ - c_-)/2$ [1,57,58]. Using these definitions (11)–(13) can be rewritten as

$$\frac{\partial c}{\partial t} = \nabla \cdot (\nabla c + \rho \nabla \phi), \tag{19}$$

$$\frac{\partial \rho}{\partial t} = \nabla \cdot (\nabla \rho + c \nabla \phi), \tag{20}$$

$$-\epsilon^2 \nabla^2 \phi = \rho. \tag{21}$$

Throughout our discussion, we shall alternate between this formulation and Eqs. (11)–(13) depending on the context. The initial and boundary conditions for this set of equations are easily derived from (14)–(18). Here we summarize those boundary conditions that change:

$$\frac{\partial c}{\partial n} + \rho \frac{\partial \phi}{\partial n} = 0, \tag{22}$$

$$\frac{\partial \rho}{\partial n} + c \frac{\partial \phi}{\partial n} = 0, \tag{23}$$

$$c(r,\theta,\phi,t=0) = 1, \tag{24}$$

$$\rho(r,\theta,\phi,t=0) = 0. \tag{25}$$

For the remainder of this paper, we shall work primarily with dimensionless equations. On occasion, we will mention the dimensional form of various expressions and equations to help make their physical interpretation more apparent.

D. Electroneutral bulk equations

In the context of electrokinetics, it is desirable to reduce the complexity of the electrochemical transport problem by replacing the PNP equations with a simpler set of equations that treats the bulk electrolyte and the double layer as separate entities. Circuit models [1,12,16,17] have been used extensively to achieve this goal by reducing the transport problem to an electrostatics problem. However, circuit models make the rather stringent assumption that bulk concentrations remain uniform at all times. Unfortunately, at high applied electric fields, this assumption is no longer valid because concentration gradients become important [1].

In the present analysis, we consider an alternative simplification of the PNP equations that allows for bulk concentration variations. Since we are interested in colloidal systems where particle diameters are on the order of micrometers, ϵ is very small, which suggests that we consider the thin double-layer limit ($\epsilon \to 0$). In this limit, the bulk remains locally electroneutral, so it is acceptable to replace Poisson's equation with the local electroneutrality condition [38,59]

$$\sum_i z_i c_i = 0. \tag{26}$$

For the case of symmetric, binary electrolytes, (26) leads to the electroneutral Nernst-Planck equations

$$\frac{\partial c}{\partial t} = \nabla^2 c, \tag{27}$$

$$0 = \nabla \cdot (c \nabla \phi), \tag{28}$$

$$\rho = 0. \tag{29}$$

Notice that the common practice of modeling the bulk electrolyte as a linear resistor obeying Ohm's law $\nabla^2\phi=0$ arises from these equations if the concentration profile is uniform.

We emphasize that these equations only describe the electrochemical system at the macroscopic level (i.e., in the bulk region of the solution). The microscopic structure within the double layer, where local electroneutrality breaks down, is completely neglected. Therefore, any physical effects of double-layer structure can only be incorporated into the mathematical model via effective boundary conditions.

III. EFFECTIVE BOUNDARY CONDITIONS OUTSIDE THE DOUBLE LAYER

When local electroneutrality is used in place of Poisson's equation, the physical boundary conditions imposed at electrode surfaces must be modified to account for the microscopic structure within the double layer. Fortunately, in the $\epsilon \to 0$ limit, the double layer remains in quasiequilibrium, so the Gouy-Chapman-Stern (GCS) model [37] can be used to derive effective boundary conditions for the system. We emphasize that the GCS model is *not* an assumption; rather, it emerges as the leading-order approximation in an asymptotic analysis of the thin double-layer limit. (See Ref. [1] for the history of this well-known result.) Because the general form for the effective boundary conditions of locally electroneutral electrochemical systems has not been extensively discussed in the literature, we provide a detailed derivation of these boundary conditions and discuss some associated dimensionless parameters.

A. Compact-layer surface capacitance

We begin our discussion of effective boundary conditions by considering the "Stern boundary condition" (14), which describes the (linear) capacitance of a possible compact layer on the surface. Because Eq. (14) involves the electric potential and electric field at the inner edge of the diffuse charge layer, it cannot be directly used as a boundary condition for the locally electroneutral equations (27)–(29). However, by rearranging (14) and using the GCS model, it is possible to rewrite the Stern boundary condition so that it only explicitly involves the electric potential and average concentration at the macroscopic surface of the electrode (i.e., the outer edge of the diffuse charge layer) [1,57]:

$$\zeta + 2\delta\sqrt{c}\,\sinh(\zeta/2) = v - \phi. \tag{30}$$

Here ζ is the potential drop across the diffuse part of the double layer (i.e., the zeta potential), v is the potential of the metal sphere on the thermal voltage scale, and ϕ and c are the values of the electric potential and average concentration at the outer edge of the diffuse charge layer. With dimensions, (30) is given by

$$\tilde{\zeta} + 2\lambda_s\sqrt{\frac{2kTC}{\varepsilon_s}}\,\sinh\left(\frac{z_+e\bar{\zeta}}{2kT}\right) = V - \Phi \tag{31}$$

where $\bar{\zeta}$ is the dimensional zeta potential. Note that the GCS model for the double layer leads to the conclusion that the only dependence of the normal derivative of the electric potential on the double-layer structure is through the ζ-potential. A more detailed derivation of this form of the Stern boundary condition can be found in [57].

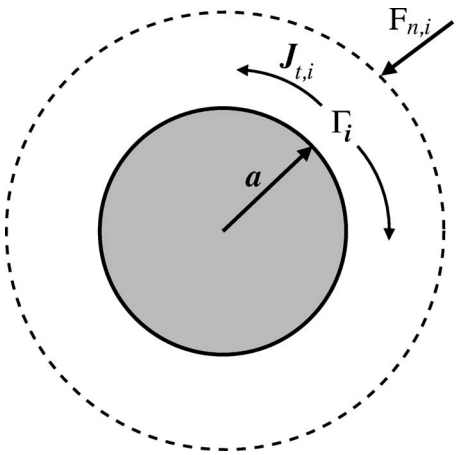

FIG. 2. Schematic diagram of normal and tangential fluxes involved in the surface conservation law (32). The shaded circle represents the metal particle; the dashed circle represents the outer "edge" of the double layer.

B. Diffuse-layer surface conservation laws

The effective boundary conditions for ionic fluxes are more complicated. Because the physical domain for the macroscopic equations (27)–(29) excludes the diffuse part of the double layer, the no-flux boundary conditions do not apply—it is possible for there to exist ion flux between the bulk region and the double layer. Moreover, there is also the possibility of ion transport within the double layer itself (often neglected) which must be accounted for.

The derivation of the effective flux boundary conditions (39) is based on a general theory of surface conservation laws at microscopically diffuse interfaces, which we develop in Ref. [48]. The basic physical idea is to integrate out the spatial variation within the double layer in the direction normal to the electrode-electrolyte interface. While intuitively obvious, carrying out the integration involves careful use of asymptotic analysis to address the mathematical subtleties of integration over boundary layers. The theory tells us that effective flux boundary conditions have the physically apparent form

$$\frac{\partial\Gamma_i}{\partial t} = -\nabla_s\cdot\mathbf{J}_{t,i} + F_{n,i} \tag{32}$$

where $(\nabla_s\cdot)$ denotes surface divergence, $\mathbf{J}_{t,i}$ is the tangential flux within, and $F_{n,i}$ is the normal flux into the boundary layer (see Fig. 2). The effective fluxes $\mathbf{J}_{t,i}$ and $F_{n,i}$ are directly related to the flux $\mathbf{F}_i$ for the transport process via

$$\mathbf{J}_{t,i} = \epsilon\int_0^\infty (\tilde{\mathbf{F}}_{t,i} - \hat{\mathbf{F}}_{t,i})dz, \tag{33}$$

$$F_{n,i} = \mathbf{F}_i \cdot \hat{n}, \tag{34}$$

where $\tilde{\mathbf{F}}$ and $\hat{\mathbf{F}}$ denote the flux within the boundary layer and the flux in the bulk just outside the boundary layer and the integration is over the entire boundary layer (i.e., z is the inner variable of a boundary-layer analysis). For electrochemical transport, the flux is given by the Nernst-Planck equation

$$\mathbf{F}_i = -(\boldsymbol{\nabla} c_i + z_i c_i \boldsymbol{\nabla} \phi). \tag{35}$$

Substituting this expression into (33) and (34), rearranging a bit, and using the definition of a surface excess concentration [39,40,48]

$$\Gamma_i \equiv \epsilon \int_0^\infty \gamma_i \, dz = \epsilon \int_0^\infty (\tilde{c}_i - \hat{c}_i) dz, \tag{36}$$

we obtain

$$\mathbf{J}_{t,i} = -\left(\boldsymbol{\nabla}_s \Gamma_i + z_i \Gamma_i \boldsymbol{\nabla}_s \hat{\phi} + \epsilon z_i \int_0^\infty \tilde{c}_i \boldsymbol{\nabla}_s \tilde{\psi} \, dz \right), \tag{37}$$

$$F_{n,i} = -\frac{\partial c_i}{\partial n} - z_i c_i \frac{\partial \phi}{\partial n}, \tag{38}$$

where $\tilde{\psi} \equiv \tilde{\phi} - \hat{\phi}$ is the excess electric potential within the boundary layer and $\boldsymbol{\nabla}_s$ denotes a surface gradient. As before, the tilde and caret accents denote the quantities within the boundary layer and in the bulk immediately outside the boundary layer. Finally, the effective flux boundary conditions for electrochemical transport follow by using these results in (32):

$$\frac{\partial \Gamma_i}{\partial t} = \boldsymbol{\nabla}_s \cdot \left(\boldsymbol{\nabla}_s \Gamma_i + z_i \Gamma_i \boldsymbol{\nabla}_s \phi + \epsilon z_i \int_0^\infty \tilde{c}_i \boldsymbol{\nabla}_s \tilde{\psi} \, \mathrm{d}z \right) - \left(\frac{\partial c_i}{\partial n} + z_i c_i \frac{\partial \phi}{\partial n} \right). \tag{39}$$

Note that even though our choice of electric potential scale eliminates the need to explicitly refer to the ionic charge numbers z_i, we opt to continue using them in the present discussion so that it is clear where the charge number should appear for alternative choices of the electric potential scale; in the following discussion, the z_i are essentially the sign of the "dimensional" ionic charge numbers.

There are a few important features of (39) worth mentioning. First, the surface transport term (first term on the right-hand side) does not always contribute to the leading-order effective flux boundary condition. Whether the surface conduction term must be retained at leading order depends on the magnitude of Γ_i (which in turn depends on the ζ potential) and the tangential component of the bulk electric field. Interestingly, when the surface transport term is significant, the flux boundary condition depends explicitly on the small parameter ϵ. Also, (39) allow for two important physical effects that only arise for two- (2D) and three-dimensional (3D) systems: (i) nonuniform double-layer charging and (ii) surface transport within the double layer itself. The presence of these effects lead to richer behavior for 2D and 3D systems compared to the 1D system studied in [1].

To put (39) into a more useful form, we use the GCS model of the double layer to express the surface flux densities in terms of the ζ potential and the bulk concentration. From the GCS model [37,38], we know that the excess concentration of each ionic species is given by

$$\gamma_i = \tilde{c}_i - \hat{c}_i = \hat{c}(e^{-z_i \tilde{\psi}} - 1) \tag{40}$$

and that

$$\frac{\partial \tilde{\psi}}{\partial z} = -2\sqrt{\hat{c}} \sinh\left(\frac{z_+ \tilde{\psi}}{2} \right). \tag{41}$$

Using these expressions, it is straightforward to show that the surface excess concentration is

$$\Gamma_i = \frac{2\epsilon\sqrt{\hat{c}}}{|z_i|}(e^{-z_i \zeta/2} - 1). \tag{42}$$

Therefore, the first two surface flux density terms in (39) can be written as

$$\boldsymbol{\nabla}_s \Gamma_i + z_i \Gamma_i \boldsymbol{\nabla}_s \hat{\phi} = \frac{\Gamma_i}{2} \boldsymbol{\nabla}_s \ln \hat{c} + z_i \Gamma_i \boldsymbol{\nabla}_s \hat{\phi} - \epsilon \, \mathrm{sgn}(z_i) \sqrt{\hat{c}} e^{-z_i \zeta/2} \boldsymbol{\nabla}_s \zeta. \tag{43}$$

To evaluate the last term in the surface flux density, we observe that

$$\boldsymbol{\nabla}_s \tilde{\psi} = \frac{\partial \tilde{\psi}}{\partial z} \left(-\frac{\boldsymbol{\nabla}_s \zeta}{2\sqrt{\hat{c}} \sinh(\zeta/2)} + \frac{z}{2} \boldsymbol{\nabla}_s \ln \hat{c} \right), \tag{44}$$

which follows directly by comparing the normal and surface derivatives of the leading-order expression for the electric potential within the double layer [1,57,58]

$$\tilde{\psi}(z) = 4 \tanh^{-1}[\tanh(\zeta/4) e^{-\sqrt{\hat{c}} z}]. \tag{45}$$

Using this result, the integral in (39) greatly simplifies and yields

$$\epsilon z_i \int_0^\infty \tilde{c}_i \boldsymbol{\nabla}_s \tilde{\psi} \, dz = \epsilon \, \mathrm{sgn}(z_i) \sqrt{\hat{c}} e^{-z_i \zeta/2} \boldsymbol{\nabla}_s \zeta + \frac{\Gamma_i}{2} \boldsymbol{\nabla}_s \ln \hat{c}. \tag{46}$$

Finally, combining (43) and (46), the effective flux boundary condition (39) becomes

$$\frac{\partial \Gamma_i}{\partial t} = \boldsymbol{\nabla}_s \cdot (\Gamma_i \boldsymbol{\nabla}_s \ln \hat{c} + z_i \Gamma_i \boldsymbol{\nabla}_s \hat{\phi}) - \left(\frac{\partial c_i}{\partial n} + z_i c_i \frac{\partial \phi}{\partial n} \right) \tag{47}$$

where (dropping carets) c and ϕ are understood to be in the bulk, just outside the double layer. Notice that the tangential gradients in the ζ potential have vanished in this equation so that the surface flux density of the individual species is independent of $\boldsymbol{\nabla}_s \zeta$.

In terms of the (dimensionless) chemical potentials of the ions,

$$\mu_i = \ln c_i + z_i \hat{\phi}, \tag{48}$$

the surface conservation law (47) reduces to a very simple form,

$$\frac{\partial \Gamma_i}{\partial t} = \nabla_s \cdot (\Gamma_i \nabla \mu_i) - \hat{n} \cdot c_i \nabla \mu_i \tag{49}$$

where it is clear that the tangential gradient in the *bulk* chemical potential just outside the double layer drives the transport of the *surface* excess concentration of each ion, as well as the bulk transport. This form of the surface conservation law should hold more generally, even when the chemical potential does not come from dilute solution theory (PNP equations).

Effective boundary conditions similar to (47) describing the dynamics of the double layer have been known for some time. In the late 1960s, Dukhin, Deryagin, and Shilov essentially used (47) in their studies of surface conductance and the polarization of the diffuse charge layer around spherical particles with thin double layers at weak applied fields [42,45,47]. Later, Hinch *et al.* used similar boundary conditions in their extension of the work of Dukhin *et al.* to explicitly calculate the tangential flux terms for a range of large surface potentials and asymmetric electrolytes [43,44]. A key feature of both of these studies is the focus on small deviations from bulk equilibrium. As a result, the effective boundary conditions used are basically applications of (47) for weak perturbations to the background concentration and electric potential. Our work differs from these previous analyses because we do not require that the bulk concentration only weakly deviates from a uniform profile, and we more rigorously justify the approximation through the use of matched asymptotics. In addition, our analysis is not restricted to the use of the GCS model for the double layer; Eqs. (37)–(39) are valid even for more general models of the boundary layer.

Before moving on, we write the effective boundary conditions in dimensional form to emphasize their physical interpretation:

$$\frac{\partial \bar{\Gamma}_i}{\partial t} = \nabla_s \cdot \left[D \bar{\Gamma}_i \nabla_s \ln\left(\frac{C}{C_0}\right) + \frac{z_i e D}{kT} \bar{\Gamma}_i \nabla_s \Phi \right] - \left(D_i \frac{\partial C_i}{\partial n} + \frac{z_i e D}{kT} C_i \frac{\partial \Phi}{\partial n} \right), \tag{50}$$

where $\bar{\Gamma}_i$ is the dimensional surface excess concentration of species i and is defined as

$$\bar{\Gamma}_i \equiv \int_{dl} (\tilde{C}_i - C_i) dZ \tag{51}$$

where the integration is only over the double layer. With the units replaced, it becomes clear that the effective boundary condition is a two-dimensional conservation law for the excess surface concentration Γ_i with a driving force for the flux and a source term that depend only on the dynamics away from the surface. Thus, the effective boundary conditions naturally generalize the simple capacitor picture of the double layer to allow for flow of ionic species tangentially along the electrode surface.

C. Surface charge and excess salt concentration

Since the governing equations (27)–(29) are formulated in terms of the salt concentration and charge density, it is convenient to derive boundary conditions that are directly related to these quantities. Toward this end, we define ϵq and ϵw to be the surface charge density and surface excess salt concentration, respectively:

$$q = \int_0^\infty \tilde{\rho}\, dz = \frac{1}{2} \int_0^\infty (\gamma_+ - \gamma_-) dz, \tag{52}$$

$$w = \int_0^\infty (\tilde{c} - \hat{c}) dz = \frac{1}{2} \int_0^\infty (\gamma_+ + \gamma_-) dz. \tag{53}$$

By integrating the expressions for the diffuse-layer salt concentration and charge density [1,37–39],

$$\tilde{c} = \hat{c} \cosh \tilde{\psi}, \tag{54}$$

$$\tilde{\rho} = -\hat{c} \sinh \tilde{\psi}, \tag{55}$$

and using (41), both q and w can be expressed as simple functions of the ζ potential and the bulk concentration just outside the double layer:

$$q = -2\sqrt{\hat{c}} \sinh(\zeta/2), \tag{56}$$

$$w = 4\sqrt{\hat{c}} \sinh^2(\zeta/4). \tag{57}$$

Thus, we can combine the effective flux boundary conditions for individual ions (39) to obtain

$$\epsilon \frac{\partial q}{\partial t} = \epsilon \nabla_s \cdot \left(\nabla_s q + w \nabla_s \hat{\phi} + \int_0^\infty \tilde{c} \nabla_s \tilde{\psi}\, dz \right) - c \frac{\partial \phi}{\partial n}, \tag{58}$$

$$\epsilon \frac{\partial w}{\partial t} = \epsilon \nabla_s \cdot \left(\nabla_s w + q \nabla_s \hat{\phi} + \int_0^\infty \rho \nabla_s \tilde{\psi}\, dz \right) - \frac{\partial c}{\partial n}. \tag{59}$$

Notice that, as in the PNP equations written in terms of c and ρ, there is a symmetry between q and w in these equations. As in the previous section, we can use the GCS model to rewrite (58) and (59) solely in terms of bulk field variables and the ζ potential:

$$\epsilon \frac{\partial q}{\partial t} = \epsilon \nabla_s \cdot \left(q \nabla_s \ln \hat{c} + w \nabla_s \hat{\phi} \right) - c \frac{\partial \phi}{\partial n}, \tag{60}$$

$$\epsilon \frac{\partial w}{\partial t} = \epsilon \nabla_s \cdot \left(w \nabla_s \ln \hat{c} + q \nabla_s \hat{\phi} \right) - \frac{\partial c}{\partial n}, \tag{61}$$

which is the form of the effective flux boundary conditions we shall use in our analysis below.

IV. SURFACE TRANSPORT PROCESSES

Before proceeding to the analysis, we discuss the relative importance of the various surface transport processes, com-

TABLE II. Summary of surface flux formulas for electrochemical transport.

	Dimensional formula[a]	Dimensionless formula
$\mathbf{J}_{t,\pm}$	$-b\Gamma_\pm \nabla_s \mu_\pm$	$-\Gamma_\pm \nabla_s \mu_\pm$
	$-\left(D\Gamma_\pm \nabla_s \ln(C/C_0) \pm \frac{z_+ eD}{kT}\Gamma_\pm \nabla_s \Phi\right)$	$-(\Gamma_\pm \nabla_s \ln c \pm \Gamma_\pm \nabla_s \phi)$
$\mathbf{J}^{(d)}_{t,\pm}$	$-D\Gamma_\pm \nabla_s \ln (C/C_0)$	$-\Gamma_\pm \nabla_s \ln c$
$\mathbf{J}^{(e)}_{t,\pm}$	$\mp \frac{z_+ eD}{kT}\Gamma_\pm \nabla_s \Phi$	$\mp \Gamma_\pm \nabla_s \phi$
$\mathbf{J}_{t,q}$	$-\left(DQ\nabla_s \ln(C/C_0) + \frac{z_+ eD}{kT} W \nabla_s \Phi\right)$	$-\epsilon(q\nabla_s \ln c + w\nabla_s \phi)$
$\mathbf{J}^{(d)}_{t,q}$	$-DQ\nabla_s \ln(C/C_0)$	$-\epsilon q \nabla_s \ln c$
$\mathbf{J}^{(e)}_{t,q}$	$-\frac{z_+ eD}{kT} W \nabla_s \Phi$	$-\epsilon w \nabla_s \phi$
$\mathbf{J}_{t,w}$	$-\left(DW\nabla_s \ln(C/C_0) + \frac{z_+ eD}{kT} Q \nabla_s \Phi\right)$	$-\epsilon(w\nabla_s \ln c + q\nabla_s \phi)$
$\mathbf{J}^{(d)}_{t,w}$	$-DW\nabla_s \ln c(C/C_0)$	$-\epsilon w \nabla_s \ln c$
$\mathbf{J}^{(e)}_{t,w}$	$-\frac{z_+ eD}{kT} Q \nabla_s \Phi$	$-\epsilon q \nabla_s \phi$

[a]We have abused notation and used the same variable Γ_i for both the dimensional and dimensionless formulas. Γ_i in the dimensional formulas is equal to $C_0 a \Gamma_i$ in the dimensionless formulas, the dimensional surface charge density Q is defined by $Q \equiv C_0 \lambda_D q$, and the dimensional excess neutral salt concentration W is defined by $W \equiv C_0 \lambda_D w$.

pared to their neutral bulk counterparts. For clarity, we summarize our results for tangential surface fluxes in Table II, with and without dimensions. As with the associated bulk fluxes summarized in Table I, we introduce different notations for contributions by diffusion and electromigration [superscripts (d) and (e), respectively] to the tangential (subscript t) surface fluxes of cations, anions, charge, and neutral salt (subscripts $+$, $-$, q, and w, respectively). This allows us to define dimensionless parameters comparing the various contributions.

Bikerman pioneered the experimental and theoretical study of double-layer surface transport [60,61] and first defined the dimensionless ratio of surface current to bulk current, across a geometrical length scale a, for a uniformly charged double layer and a uniform bulk solution [46]. Using our notation, the Bikerman number is

$$\mathrm{Bi} = \frac{J_{t,q}}{aJ_0} \tag{62}$$

where $J_0 = z_+ eF_0$ is a reference bulk current in terms of the typical diffusive flux $F_0 = DC_0/a$. Deryagin and Dukhin later added contributions from electro-osmotic flow, using the GCS model of the double layer (as did Bikerman) [47], and Dukhin and collaborators then used this model to study electrophoresis of highly charged particles (with large but nearly uniform surface charge) [42,45,53]. As in other situations, surface conduction effects in electrophoresis are controlled by Bi, which thus came to be known in the Russian literature as the "Dukhin number" Du. (Dukhin himself denoted it by Rel.)

Recently, Bazant, Thornton, and Ajdari pointed out that the (steady) Bikerman-Dukhin number is equal to the ratio of the excess surface salt concentration to its bulk counterpart at the geometrical scale a,

$$\mathrm{Bi} = \frac{\Gamma_+ + \Gamma_i}{2aC_0}, \tag{63}$$

and they showed its importance in a one-dimensional problem of electrochemical relaxation between parallel-plate electrodes [1]. This surprising equivalence (in light of the definition of Bi) demonstrates that surface conduction becomes important relative to bulk conduction simply because a significant number of ions are adsorbed in the double layer compared to the nearby bulk solution. This means that salt adsorption leading to bulk diffusion should generally occur at the same time as surface conduction, if the double layer becomes highly charged during the response to an applied field or voltage, as in our model problems below.

Unlike prior work, however, our multidimensional nonlinear analysis allows for nonuniform, time-dependent charging of the double layer, so the Bikerman-Dukhin number can only be defined locally and in principle could vary wildly across the surface. Moreover, since we separate the contributions to surface transport from diffusion and electromigration, we can define some new dimensionless numbers. From Eqs. (60) and (61), we find that the following surface-to-bulk flux ratios are related to the excess surface-to-bulk ratio of neutral salt concentration:

$$\alpha = \epsilon w = 4\frac{\lambda_D}{a}\sqrt{\frac{C}{C_0}}\sinh^2\left(\frac{z_+ e\bar{\zeta}}{4kT}\right) \tag{64}$$

$$\sim \frac{|J^{(e)}_{t,q}|}{aJ_0} \sim \frac{|J^{(d)}_{t,w}|}{aF_0}. \tag{65}$$

Note that when surface diffusion is neglected, as in most prior work, then $\alpha = \mathrm{Bi}$, since surface currents arise from electromigration alone. The other surface-to-bulk flux ratios are given by the surface-to-bulk ratio of the charge density,

$$\beta = \epsilon|q| = 2\frac{\lambda_D}{a}\sqrt{\frac{C}{C_0}}\sinh\left(\frac{z_+ e\bar{\zeta}}{2kT}\right) \tag{66}$$

$$\sim \frac{|J_{t,q}^{(d)}|}{aJ_0} \sim \frac{|J_{t,w}^{(e)}|}{aF_0}. \tag{67}$$

For thin double layers ($\lambda_D \ll a$), we see that the surface-to-bulk flux ratios α and β are only significant when $\bar{\zeta}$ significantly exceeds the thermal voltage kT/e.

To better understand how the charge and neutral salt fluxes are carried, it is instructive to form the ratio of these numbers,

$$\frac{\alpha}{\beta} = \tanh\left(\frac{z_+ e\bar{\zeta}}{4kT}\right) \tag{68}$$

$$\sim \frac{|J_{t,w}^{(d)}|}{|J_{t,w}^{(e)}|} \sim \frac{|J_{t,q}^{(e)}|}{|J_{t,q}^{(d)}|}. \tag{69}$$

For weakly charged double layers, $z_+ e\bar{\zeta} \ll 4kT$, where $\alpha \ll \beta$, the (small) surface flux of salt is dominated by electromigration, while the surface flux of charge (surface current) is dominated by diffusion (if bulk concentration gradients exist). For highly charged double layers $z_+ e\bar{\zeta} > 4kT$ where $\alpha \sim \beta$, the contributions to each flux by diffusion and electromigration become comparable, as counterions are completely expelled ($q \sim w$).

V. NONLINEAR STEADY RESPONSE FOR THIN DOUBLE LAYERS

A. Effective equations

Using the mathematical model developed in the previous section, we now examine the steady response of a metal sphere or cylinder with thin double layers subjected to a large, uniform applied electric field. At steady state, the unsteady term is eliminated from the governing equations (27)–(29), so we have

$$0 = \nabla^2 c, \tag{70}$$

$$0 = \nabla \cdot (c\nabla\phi). \tag{71}$$

Similarly, the flux boundary conditions (60) and (61) become

$$0 = \epsilon\nabla_s \cdot (q\nabla_s \ln c + w\nabla_s\phi) - c\frac{\partial\phi}{\partial n}, \tag{72}$$

$$0 = \epsilon\nabla_s \cdot (w\nabla_s \ln c + q\nabla_s\phi) - \frac{\partial c}{\partial n}. \tag{73}$$

Notice that we have retained the surface transport terms in these boundary conditions even though they appear at $O(\epsilon)$. At large applied fields, it is no longer valid to order the terms in an asymptotic expansion by ϵ alone. We also need to consider factors of the form ϵe^{ζ} or $\epsilon \sinh(\zeta)$ since e^{ζ} may be as large as $O(1/\epsilon E)$ for large applied fields. Since both q and w contain factors that grow exponentially with the ζ potential, we cannot discard the surface conduction terms in (72) and (73). Finally, the Stern boundary condition (30) remains unchanged because it does not involve any time derivatives.

As mentioned earlier, the steady problem exhibits interesting features that have not been extensively explored. Unfortunately, the nonlinearities present in the governing equations and boundary conditions make it difficult to proceed analytically, so we use numerical methods to gain insight into the behavior of the system. In this section, we first briefly describe the numerical model we use to study the system. We then use the numerical model to study the development of $O(1)$ bulk concentration variations and their impact on transport around metal colloid spheres.

B. Numerical model

To solve (70) and (71) numerically in a computationally efficient manner, we use a pseudospectral method [62–64]. For problems in electrochemical transport, pseudospectral methods are particularly powerful because they naturally resolve boundary layers by placing more grid points near boundaries of the physical domain [62–64]. We further reduce the computational complexity and cost of the numerical model by taking advantage of the axisymmetry of the problem to reduce the numerical model to two dimensions (as opposed to using a fully 3D description).

For the computational grid, we use a tensor product grid of a uniformly spaced grid for the polar angle direction and a shifted semi-infinite rational Chebyshev grid for the radial direction [63]. To obtain the discretized form of the differential operators on this grid, we use Kronecker products of the differentiation matrices for the individual one-dimensional grids [62]. The numerical model is then easily constructed using collocation by replacing field variables and continuous operators in the mathematical model by grid functions and discrete operators. The resulting nonlinear, algebraic system of equations for the values of the unknowns at the grid points is solved using a standard Newton iteration with continuation in the strength of the applied electric field. The Jacobian for the Newton iteration is computed exactly by using a set of simple matrix-based differentiation rules derived in the Appendix of [59]. By using the exact Jacobian, the convergence rate of the Newton iteration is kept low; typically less than five iterations are required for each value of the continuation parameter before the residual of the solution to the discrete system of equations is reduced to an absolute tolerance of 10^{-8}.[2] Directly computing the Jacobian in matrix form had the additional advantage of making it easy to implement the numerical model in MATLAB, a high-level programming language with a large library of built-in functions. It is also worth mentioning that we avoid the problem of dealing with infinite values of the electric potential by formulating the numerical model in terms of $\phi + Er\cos\theta$, the deviation of the electric potential from that of the uniform applied electric field, rather than ϕ itself.

[2]The residual is computed using the L^{∞} norm.

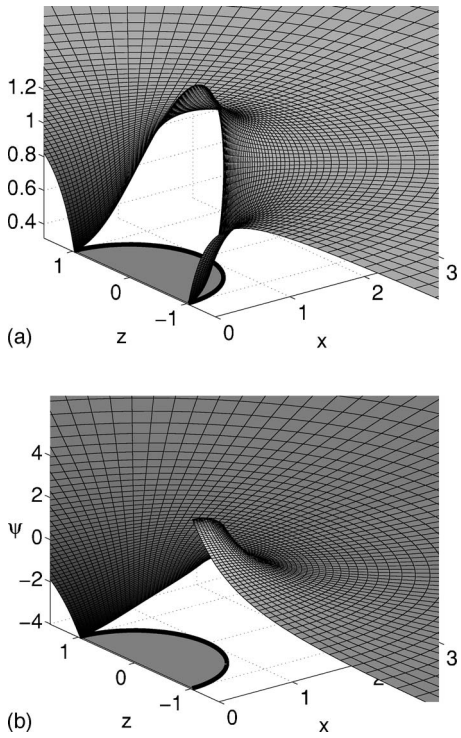

FIG. 3. Numerical solutions for the concentration c (top) and excess electric potential ψ (bottom) for $E=10$, $\epsilon=0.01$, $\delta=1$. Notice the large gradients in the concentration profile near the surface of the sphere.

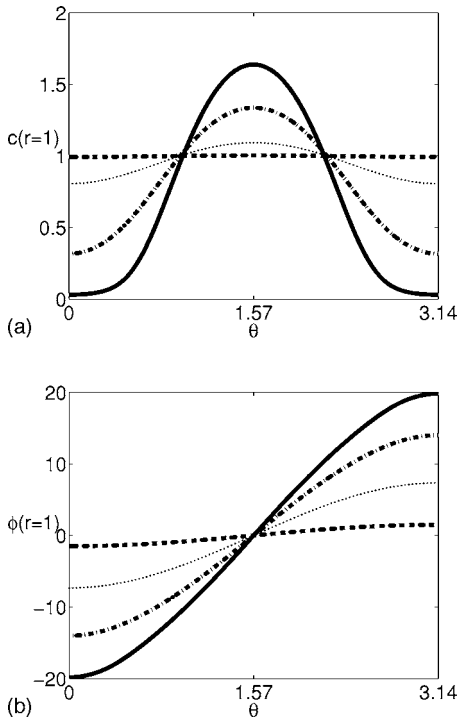

FIG. 4. Bulk concentration $\hat{c}$ and electric potential $\hat{\phi}$ at the surface of the sphere for varying values of the applied electric field. In these figures, $\epsilon=0.01$ and $\delta=1$. Notice that for $E=15$, the poles ($\theta=0$ and $\theta=\pi$) are about to be depleted of ions (i.e., $\hat{c}\approx 0$).

In our numerical investigations, we used the numerical method described above with 90 radial and 75 angular grid points. This grid resolution balanced the combined goals of high accuracy and good computational performance. Figure 3 shows typical solutions for the concentration and electric potential (relative to the background applied potential) for large applied electric fields. A comparison of the concentration and electric potential at the surface of the sphere for varying values of E is shown in Fig. 4.

C. Enhanced surface excess concentration and surface conduction

Perhaps the most important aspects of the steady response at high applied electric fields are the enhanced surface excess ion concentration and surface transport within the double layer. As shown in Fig. 5, at high applied fields, the excess surface concentrations is $O(1/E)$, so surface transport within the double layer (shown in Fig. 6) becomes non-negligible in the leading-order effective flux boundary conditions (72) and (73). Interestingly, surface conduction, $\mathbf{J}_{t,q}^{(e)}$, and $\mathbf{J}_{t,w}^{(e)}$, are the dominant contributions to surface transport (see Fig. 7). While there are clearly surface gradients in concentration, surface diffusion is smaller than surface migration by a factor on the order of $1/\hat{c}E$. Also, we reiterate that the driving force for surface transport is solely from surface gradients of the bulk concentration and bulk electric potential; gradients in the ζ potential do not play a role because they are completely canceled out.

An important feature of the surface fluxes $\mathbf{J}_{t,q}$ and $\mathbf{J}_{t,w}$ shown in Fig. 6 is that they are nonuniform. This nonuniformity is strongly influenced by the nonuniformity in the tangential electric field (see Fig. 8). The nonuniformity of the surface excess salt concentration and charge surface density also play a role but to a lesser extent. For the steady problem, the surface excess concentration of ions remains constant in time, so the nonuniformity in the surface fluxes leads to nonuniform normal fluxes of current and neutral salt from the bulk into the double layer (see Fig. 9). Notice that the normal flux of neutral salt into the double layer, which is given by $-\partial c/\partial n$, shows an injection of neutral salt at the poles ($-\partial c/\partial n>0$), where the charging is strongest, and an ejection of neutral salt at the equator ($-\partial c/\partial n<0$), where there is essentially no excess neutral salt buildup. This configuration of fluxes leads to the neutral salt depletion at the poles and accumulation at the equator shown in Figs. 3 and 4. Similarly, the normal current density $-\hat{c}\,\partial\phi/\partial n$ shows an influx of negative (positive) current density at the north (south) pole and a positive (negative) current density closer to the equator. At the equator, there is no normal current density because the normal diffusion currents of cations and anions exactly balance and there is no normal electric field to drive a migration current.

D. Bulk diffusion and concentration gradients

One major consequence of surface conduction is transport of large amounts of neutral salt into the double layer. These cause strong concentration gradients to appear near the sur-

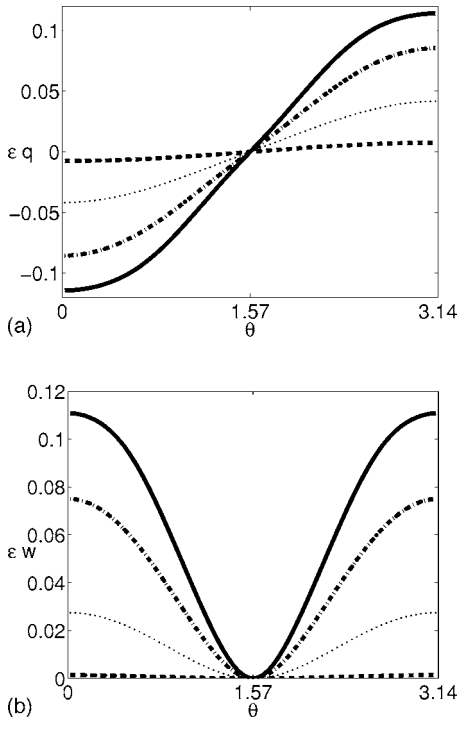

FIG. 5. Surface charge density ϵq (top) and excess surface concentration of neutral salt ϵw (bottom) and for varying values of the applied electric field. In these figures, $\epsilon=0.01$ and $\delta=1$. Notice that for large applied fields, $\epsilon w=O(1/E)$ and $\epsilon q=O(1/E)$ so that the surface conduction terms in (60) and (61) are $O(1)$.

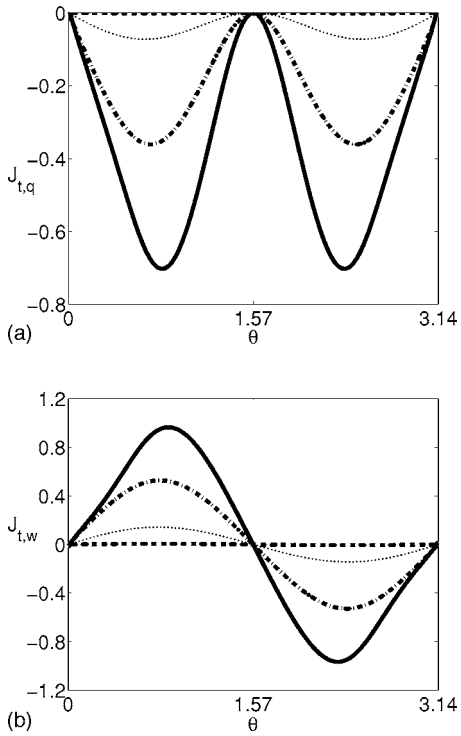

FIG. 6. Tangential surface fluxes for the surface charge density $|\mathbf{J}_{t,q}|$ (top) and excess surface concentration of neutral salt $|\mathbf{J}_{t,w}|$ (bottom) for varying values of the applied electric field. In these figures, $\epsilon=0.01$ and $\delta=1$. Notice that for large applied fields, the surface fluxes are $O(1)$ quantities and make a non-negligible leading-order contribution in (60) and (61).

face of the sphere (Figs. 3 and 4), indicating that the usual assumption of a uniform concentration profile is invalid at high electric fields. The presence of these large concentration gradients at relatively low electric fields ($E\approx 5$) should not be surprising since it is well known that large voltage effects often begin with voltages as low as a few times the thermal voltage [1]. The dramatic influence of the voltage arises from the exponential dependence of double-layer concentrations on the ζ potential.

Since the transport of neutral salt is driven by concentration gradients, the presence of these strong variations leads to diffusion currents (see Fig. 10). An important feature of these diffusion currents is that they are closed; current lines start on the surface of the sphere near the equator where neutral salt is ejected into the bulk (as a result of neutral salt transport within the double layer) and end close to the poles where neutral salt is absorbed by the double layer. These recirculation currents are important because they allow the system to conserve the total number of cations and anions *locally*. Without them, the local depletion and accumulation of ions would require global changes to the bulk concentration (i.e., the concentration at infinity would be affected).

While the presence of diffusion currents is interesting, we must be careful in how they are interpreted in terms of the motion of individual ion molecules. In actuality, no ions are moving purely under the influence of diffusion. Rather, the cation and anion migration flux densities are slightly imbalanced due to the presence of a concentration gradient which results in a net transport of neutral salt concentration.

E. Individual ion currents

Since cations and anions are the physical entities that are transported through the electrolyte, it is useful to consider the cation and anion flux densities individually. As shown in Fig. 11, in the bulk, the contribution of electromigration to transport dominates diffusion. Moreover, within a short distance from the sphere, the electromigration term itself becomes dominated by the contribution from the applied electric field. Thus, the concentration gradient only serves to slightly bias the flux densities so that cation (anion) motion is slightly retarded near the north (south) pole.

It is more interesting to consider the surface transport of the individual ions within the double layer. In the northern hemisphere, the double layer is dominated by anions; similarly, the southern hemisphere is dominated by cations. As a result, transport in each hemisphere is primarily due to only one species (see Fig. 12). This observation provides a direct explanation for the depletion and accumulation regions in the concentration profile in terms of the motion of individual ions. As mentioned earlier, the transport is from the poles to the equator because surface conduction is driven by the tangential component of the bulk electric field (see Fig. 8). Since the double layer in the northern hemisphere is predominantly composed of anions, the surface ion transport is from the poles toward the equator. A similar argument in the southern hemisphere shows that surface transport of the majority ion is again from the poles toward the equator. Thus,

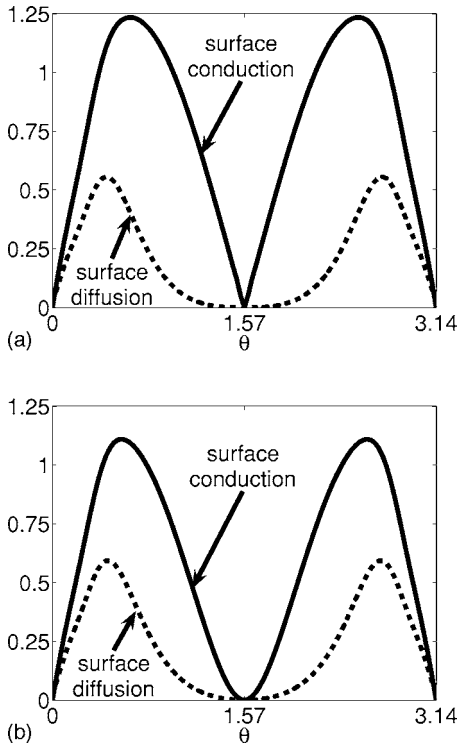

FIG. 7. Comparison of the magnitudes of $|\mathbf{J}^{(e)}|$ (solid lines) and $|\mathbf{J}^{(d)}|$ (dashed lines) for the excess surface fluxes of ϵq (top) and ϵw (bottom) for an applied electric field value of $E=15$. In these figures, $\epsilon=0.01$ and $\delta=1$. Notice that in both cases, the surface diffusion is on the order of $1/\hat{c}E$ times the surface conduction.

influx of ions into the double layer occurs in the regions near the poles and outflux occurs by the equator.

The dominance of a single species within the double layer for each hemisphere leads to a small conundrum: how does the bulk electrolyte near the surface of the sphere remain locally electroneutral? In the northern hemisphere, it would seem that more anions should be absorbed at the pole and ejected at the equator, leading to bulk charge imbalance. Analogous reasoning involving cations leads to the same conclusion in the southern hemisphere. The resolution to the conundrum comes from remembering that both diffusion and electromigration contribute to transport. The imbalance in

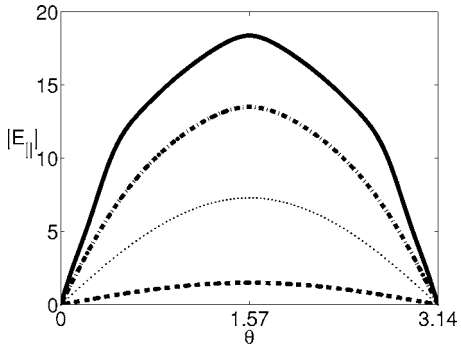

FIG. 8. Tangential component of bulk electric field $|E_t|$ at surface of sphere for varying values of the applied electric field. In this figure, $\epsilon=0.01$ and $\delta=1$.

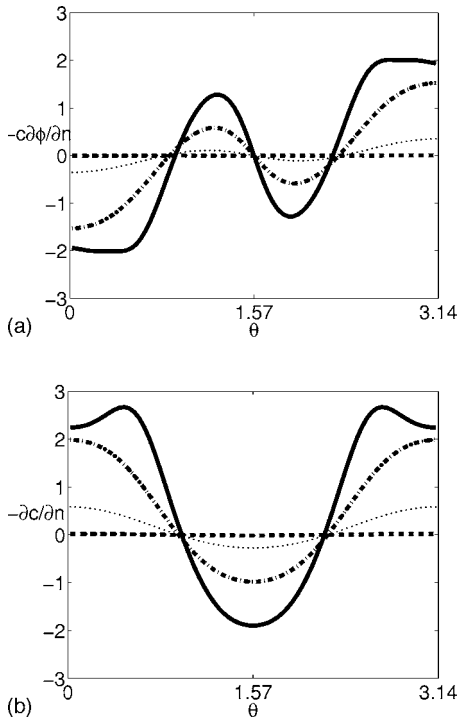

FIG. 9. Normal flux of current $c\partial\phi/\partial n$ (top) and neutral salt $\partial c/\partial n$ (bottom) into the double layer for varying values of the applied electric field. In these figures, $\epsilon=0.01$ and $\delta=1$.

the normal flux required to sustain an imbalanced concentration profile in the double layer is achieved by carefully balancing diffusion (which drives both species in the same direction) and electromigration (which drives the two species in opposite directions) so that the normal flux of the appropriate species dominates. For example, at the north pole, an electric field pointing away from the surface of the sphere will suppress the cation normal flux toward the surface while enhancing the anion normal flux.

In this situation, the electric field plays a similar role as the diffusion potential for electrochemical transport in an electroneutral solution. Recall that when the cation and anion have different diffusivities, the electric field acts to slow

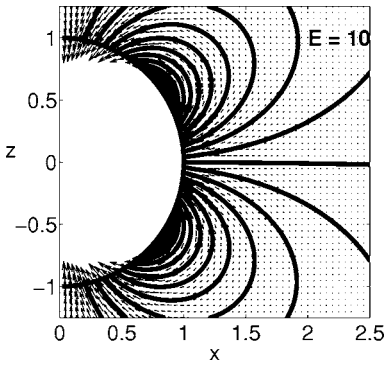

FIG. 10. Diffusion currents drive transport of neutral salt near the surface of the sphere. In this figure, $E=10$, $\epsilon=0.01$, and $\delta=1$. Notice that streamlines of neutral salt are closed; current lines start on the surface of the sphere near the equator and end closer to the poles.

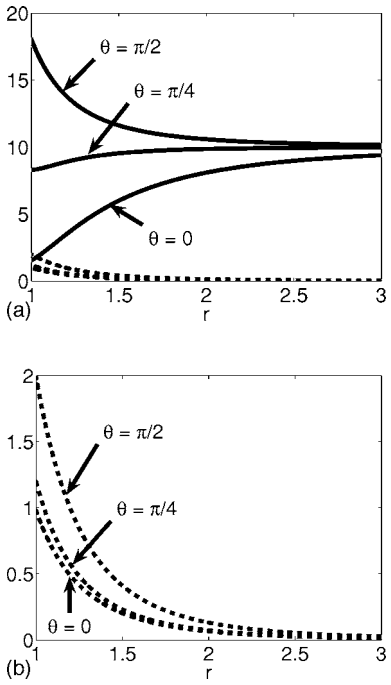

FIG. 11. Comparison of the magnitudes of bulk electromigration $|\mathbf{F}_{\rho}^{(e)}|$ (solid lines) and diffusion $|\mathbf{F}_{c}^{(d)}|$ (dashed lines) fluxes as a function of distance from the surface of the sphere at $\theta=0, \pi/4$, and $\pi/2$ (top). The figure on the bottom zooms in on the diffusion flux. In these figure, $E=10$, $\epsilon=0.01$, and $\delta=1$. Notice that the magnitude of the electromigration dominates diffusion and that the electromigration term itself becomes dominated by the contribution from the applied electric field a short distance from the surface of the sphere.

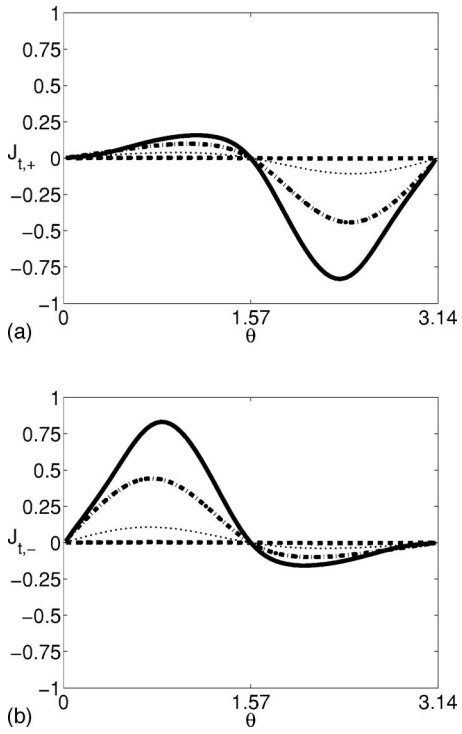

FIG. 12. Tangential surface fluxes for the cation $|\mathbf{J}_{t,+}|$ (top) and anion $|\mathbf{J}_{t,-}|$ (bottom) for varying values of the applied electric field. In these figures, $\epsilon=0.01$ and $\delta=1$. Notice that for large applied fields, the surface fluxes are $O(1)$ quantities (in the appropriate hemisphere) which leads to a non-negligible leading-order contribution in (47).

down the species with the higher diffusivity and speed up the species with the lower diffusivity in such a way that both species have equal flux densities. In the current situation, the electric field serves to create the necessary imbalance in the cation and anion flux densities so that the surface excess concentrations within the double layer can be maintained while preserving local electroneutrality in the bulk.

VI. LINEAR RELAXATION FOR ARBITRARY DOUBLE-LAYER THICKNESS

A. Debye-Falkenhagen equation

Although the focus of this paper is on nonlinear relaxation, leading to the steady state described in the previous section, it is instructive to first consider the linear response to a weak applied field, where exact solutions are possible. Moreover, the linear analysis also has relevance for the early stages of nonlinear relaxation before significant double-layer charge has accumulated, such that $\max\{\zeta(\theta)\}\ll kT/e$, as long as the metal surface is uncharged when the field is applied. The linear response also allows a more general analysis, including ac periodic response, in addition to our model problem with sudden dc forcing.

When the potential drop across the particle is much smaller than the thermal voltage ($E_0\ll 1$), it is possible to analyze the response of the system *without* assuming that the double layers are thin; that is, we need not assume that ϵ is small and may describe the system using the full unsteady PNP equations (19)–(23). Instead, we assume that the response of the system is only a small deviation from the equilibrium solution:

$$c \equiv 1, \quad \rho \equiv 0, \quad \phi = Er\cos\theta. \tag{74}$$

In this limit, we can linearize the ionic concentrations around a uniform concentration profile so that $c=1+\delta c$. Using this expression in (20) and making use of Poisson's equation (13) to eliminate the electric potential, we find that the charge density $\rho=(c_+-c_-)/2=(\delta c_+-\delta c_-)/2$ obeys the (dimensionless) Debye-Falkenhagen equation [65]:

$$\frac{\partial\rho}{\partial t} \approx \nabla^2\rho - \frac{1}{\epsilon^2}\rho. \tag{75}$$

Similarly, the flux boundary condition corresponding to this equation reduces to

$$\frac{\partial\rho}{\partial n} + \frac{\partial\phi}{\partial n} = 0. \tag{76}$$

Note that (75) and Poisson's equation (together with the no-flux and Stern boundary conditions) are a linear system of partial differential equations. Thus, we can take advantage of integral transform techniques.

B. Transform solutions for arbitrary ϵ and δ

Since for weak applied fields, the model problem is a linear initial-value problem, it is natural to carry out the analysis using Laplace transforms in time. Transforming the Debye-Falkenhagen and Poisson equations, we obtain

$$\nabla^2 \check{\rho} = \beta^2 \check{\rho}, \tag{77}$$

$$-\epsilon^2 \nabla^2 \check{\phi} = \check{\rho}, \tag{78}$$

where

$$\beta(s)^2 = s + \frac{1}{\epsilon^2} \tag{79}$$

and the haceks are used to denote Laplace-transformed variables. Similarly, the boundary conditions become

$$\frac{\partial \check{\rho}}{\partial n} + \frac{\partial \check{\phi}}{\partial n} = 0, \tag{80}$$

$$\check{\phi} + \delta\epsilon \frac{\partial \check{\phi}}{\partial n} = \upsilon s^{-1}, \tag{81}$$

$$-\nabla \check{\phi} \to E_0 s^{-1} \quad \text{as } r \to \infty. \tag{82}$$

To solve the resulting boundary-value problem, we take advantage of the spherical geometry to write the solution in terms of spherical harmonics. Since $\check{\rho}$ satisfies the modified Helmholtz equation, we can expand it in a series with terms that are products of spherical harmonics $Y_l^m(\theta,\phi)$ and modified spherical Bessel functions $k_l(\beta r)$. Moreover, we can reduce the series to a single term

$$\check{\rho}(r,\theta,\phi) = R k_1(\beta r) Y_1^0(\theta,\phi) = R k_1(\beta r) \cos\theta \tag{83}$$

by taking into account the symmetries of the charge density: (i) axisymmetry, (ii) antisymmetry with respect to $\theta = \pi/2$, and (iii) the dipolar nature of the externally applied field. Note that we have only retained the term involving the modified spherical Bessel functions that decays as $r \to 0$ because $\check{\rho}$ vanishes at infinity. Similarly, the general solution for $\check{\phi}$ may be expressed as

$$\check{\phi}(r,\theta,\phi) = -E_0 s^{-1} r \cos\theta + A + B\frac{\cos\theta}{r^2} + C k_1(\beta r)\cos\theta, \tag{84}$$

where the first term accounts for the boundary condition on the electric field at infinity, the next two terms are the general solution to Laplace's equation possessing the required symmetries, and the last term is the particular solution to Poisson's equation. Note that we have left out the monopolar term in the potential because it is only necessary for charged spheres. Our analysis is not made any less general by neglecting this term; the case of a charged sphere in a weak applied field is handled by treating it as the superposition of a charged sphere in the absence of an applied field with an uncharged sphere subjected to an applied field.

The coefficients in (83) and (84) are determined by enforcing Poisson's equation and the boundary conditions (80) and (81). Plugging (83) and (84) into Poisson's equation (78), we obtain

$$C = -\frac{R}{(\beta\epsilon)^2}. \tag{85}$$

To apply the boundary conditions, note that on the sphere $\frac{\partial}{\partial n} = -\frac{\partial}{\partial r}\big|_{r=1}$ so that

$$\frac{\partial \check{\phi}}{\partial n} = E_0 s^{-1}\cos\theta + 2B\cos\theta + \frac{1}{(\beta\epsilon)^2}\left.\frac{\partial \check{\rho}}{\partial r}\right|_{r=1} \tag{86}$$

where the last term was obtained by using the relation between C and R. Thus, the no-flux boundary condition (80) becomes

$$\begin{aligned} 0 &= E_0 s^{-1}\cos\theta + 2B\cos\theta + \left(\frac{1}{(\beta\epsilon)^2} - 1\right)\left.\frac{\partial \check{\rho}}{\partial r}\right|_{r=1} \\ &= \left[E_0 s^{-1} + 2B + R\left(\frac{1}{(\beta\epsilon)^2} - 1\right)\beta k_1'(\beta)\right]\cos\theta \end{aligned} \tag{87}$$

Similarly, the Stern boundary condition (81) becomes

$$\begin{aligned} \upsilon s^{-1} = A + \Bigg((\delta\epsilon - 1)E_0 s^{-1} + (1 + 2\delta\epsilon)B + \frac{R}{(\beta\epsilon)^2}[-k_1(\beta) \\ + \delta\epsilon\beta k_1'(\beta)]\Bigg)\cos\theta. \end{aligned} \tag{88}$$

By independently equating the coefficients of the different spherical harmonics in (87) and (88), we obtain (after a little algebra)

$$A = \upsilon s^{-1}, \tag{89}$$

$$R = \frac{-3E_0 s^{-1}(\beta\epsilon)^2}{2k_1(\beta) + [1 - (\beta\epsilon)^2(1 + 2\delta\epsilon)]\beta k_1'(\beta)}, \tag{90}$$

$$B = -\frac{E_0 s^{-1}}{2} - \frac{R}{2}\left(\frac{1}{(\beta\epsilon)^2} - 1\right)\beta k_1'(\beta). \tag{91}$$

Finally, by writing $k_1(x)$ in terms of elementary functions [66],

$$k_1(x) = \frac{e^{-x}(x+1)}{x^2}, \tag{92}$$

we can express R as

$$R = \frac{-3E_0 s^{-1}}{e^{-\beta}\left[\left(1 + \frac{2}{\beta} + \frac{2}{\beta^2}\right)(1 + 2\delta\epsilon) - \frac{1}{(\beta\epsilon)^2}\right]}. \tag{93}$$

Following Bazant, Thornton, and Ajdari [1], we focus on times that are long relative to the Debye time [$t = O(\epsilon^2)$ in dimensionless units]. In this limit, $s \ll 1/\epsilon^2$ so that the charge density on the surface of the sphere is given by

$$\check{\rho}(r=1,\theta,s) \sim \left(\frac{-K_\rho s^{-1}}{1 + \tau_\rho s}\right)\cos\theta \tag{94}$$

with

TABLE III. Formulas for the linear response of metallic cylinders and spheres to weak applied electric fields.

	Cylinder[a]	Sphere
$\check{\rho}$	$RK_1(\beta r)\cos\theta$	$Rk_1(\beta r)\cos\theta$
$\check{\phi}$	$vs^{-1}-E_0 s^{-1} r\cos\theta+\left(\frac{B}{r}-\frac{RK_1(\beta r)}{(\beta\epsilon)^2}\right)\cos\theta$	$vs^{-1}-E_0 s^{-1} r\cos\theta+\left(\frac{B}{r^2}-\frac{Rk_1(\beta r)}{(\beta\epsilon)^2}\right)\cos\theta$
R	$\frac{-2E_0 s^{-1}(\beta\epsilon)^2}{K_1(\beta)+[1-(\beta\epsilon)^2(1+\delta\epsilon)]\beta K_1'(\beta)}$	$\frac{-3E_0 s^{-1}}{e^{-\beta}[(1+2/\beta+2/\beta^2)(1+2\delta\epsilon)-1/(\beta\epsilon)^2]}$
B	$-E_0 s^{-1}-R\left(\frac{1}{(\beta\epsilon)^2}-1\right)\beta K_1'(\beta)$	$-\frac{1}{2}E_0 s^{-1}-\frac{1}{2}R\left(\frac{1}{(\beta\epsilon)^2}-1\right)\beta k_1'(\beta)$
K_ρ	$\frac{2E_0 K_1(1/\epsilon)}{K_1(1/\epsilon)-\delta K_1'(1/\epsilon)}$	$\frac{3E_0(1+\epsilon)}{2[(1+2\delta\epsilon)(1+\epsilon)+\delta]}$
τ_ρ	$-\epsilon\left\{\frac{2\epsilon K_1(1/\epsilon)+(2+\delta\epsilon-\delta K_1'(1/\epsilon)/K_1(1/\epsilon))K_1'(1/\epsilon)+\delta K_1'{}'(1/\epsilon)}{2[K_1(1/\epsilon)-K_1'(1/\epsilon)]}\right\}$	$\epsilon\left\{\frac{(1+2\delta\epsilon)(1+\epsilon)-\delta\epsilon}{2(1+\epsilon)[(1+2\delta\epsilon)(1+\epsilon)+\delta]}\right\}$
K_q	$\frac{2E_0\epsilon K_0(1/\epsilon)}{K_1(1/\epsilon)-\delta K_1'(1/\epsilon)}$	$\frac{3E_0\epsilon}{(1+2\delta\epsilon)(1+\epsilon)+\delta}$
τ_q	$-\epsilon\left\{\frac{(\epsilon+K_0'(1/\epsilon)/K_0(1/\epsilon))K_1(1/\epsilon)+[1+2\delta\epsilon-\delta K_0'(1/\epsilon)/K_0(1/\epsilon)]K_1'(1/\epsilon)+\delta K_1'{}'(1/\epsilon)}{2[K_1(1/\epsilon)-K_1'(1/\epsilon)]}\right\}$	$\epsilon\left\{\frac{(1+2\delta\epsilon)(1+\epsilon)}{2[(1+2\delta\epsilon)(1+\epsilon)+\delta]}\right\}$

[a] θ measured from vertical axis.

$$K_\rho=\frac{3E_0(1+\epsilon)}{2\gamma}, \tag{95}$$

$$\tau_\rho=\epsilon\left(\frac{(1+2\delta\epsilon)(1+\epsilon)-\delta\epsilon}{2\gamma(1+\epsilon)}\right), \tag{96}$$

$$\gamma=(1+2\delta\epsilon)(1+\epsilon)+\delta. \tag{97}$$

Inverting the Laplace transform, we see that at long times, the charge at the surface of the sphere has an exponential relaxation with a characteristic time on the order of ϵ:

$$\rho(r=1,\theta,t)\sim -K_\rho(1-e^{-t/\tau_\rho})\cos\theta. \tag{98}$$

Note that τ_ρ is on the order of the dimensionless RC time ϵ, which is much larger than ϵ^2, the dimensionless Debye time.

To obtain the linear response of cylinders, we follow the same procedure as above. The main differences are that the series solution is written in terms of a cosine series with the radial dependence given by modified Bessel functions. Without going through the algebra, the results for cylinders are given in Table III alongside the analogous results for spheres.

C. Response to a weak, oscillatory field

Due to the close relationship between Fourier and Laplace transforms, the algebra involved in analyzing the response of the sphere to a weak, oscillatory field is almost identical to the response to a suddenly applied field. Thus, for sufficiently low frequencies ($\omega\ll 1/\epsilon^2$), we can immediately write down the response to a weak, oscillatory field of the form $E=E_0\,\mathrm{Re}(e^{i\omega t})$:

$$\rho(r=1,\theta,t)=-K_\rho\,\mathrm{Re}\left(\frac{e^{i\omega t}}{1+i\omega\tau_\rho}\right)\cos\theta. \tag{99}$$

D. Accumulated surface charge density

Because of its importance in many physical processes, the accumulated surface charge density $\check{q}$ is an interesting quantity to consider. It is easily computed from the (volume) charge density ρ by integrating it in the radial direction from $r=1$ to $r=\infty$. While the identification of this integral with a surface charge density really only makes sense in the thin double-layer limit, the accumulated surface charge density is still worth examining. Fortunately, the integral is straightforward because $k_1(z)=-k_0'(z)$ [66] and the radial dependence of the charge density is independent of the angle. Using these observations, the surface charge density is given by

$$\check{q}(\theta,s)=\frac{Rk_0(\beta)}{\beta}\cos\theta=\frac{Re^{-\beta}}{\beta^2}\cos\theta. \tag{100}$$

In the long-time limit $s\ll 1/\epsilon^2$, we find that the surface charge density has an exponential relaxation $q(\theta,t)=-K_q(1-e^{-t/\tau_q})\cos\theta$ with

$$K_q=\frac{3E_0\epsilon}{\gamma}, \tag{101}$$

$$\tau_q=\epsilon\left(\frac{(1+2\delta\epsilon)(1+\epsilon)}{2\gamma}\right). \tag{102}$$

As with ρ, we see that the characteristic relaxation time for q is on the order of the dimensionless RC time.

E. Time scales for linear response

We have seen that at long times both ρ and q relax exponentially with characteristic time scales on the order of the RC time ϵ. However, as Fig. 13 shows, the relaxation times for the two quantities are not exactly the same and have a nontrivial dependence on the diffuse layer thickness ϵ and Stern capacitance δ. Notice that for infinitely thin double

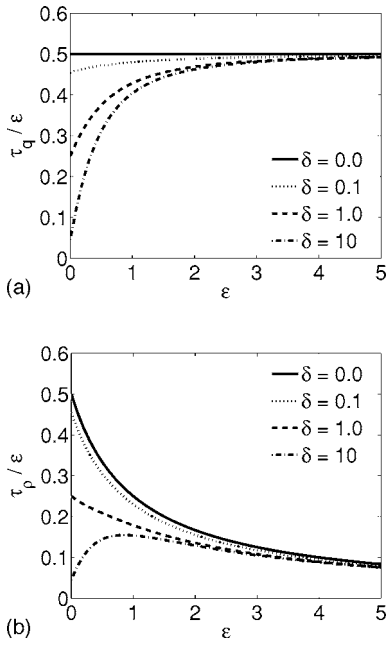

FIG. 13. Exponential relaxation time constants for the charge density ρ and the accumulated surface charge density q at weak applied fields as a function of ϵ and δ. The top panel shows the relaxation time constant for the charge density at the surface of the sphere, $\tau_\rho(r=1)$. The bottom panel shows the relaxation time constant for the accumulated surface charge density, τ_q.

layers ($\epsilon=0$) the relaxation times for the surface charge density and the accumulated charge density are identical. This behavior is expected since for thin double layers, almost all of the charge density in the diffuse layer is located very close to the surface of the particle. In this limit, the relaxation time has a strong dependence on the Stern capacitance. For thick double layers ($\epsilon \gg 1$), this dependence on the Stern capacitance disappears and the relaxation time curves for all δ values converge.

Physically, the difference in the relaxation times for the surface charge and the accumulated charge densities for nonzero ϵ values is an indication of the complex spatiotemporal structure of the double-layer charging. For thin double layers, the difference between τ_ρ and τ_q is relatively small because the charge in the double layer is restricted to a thin region. For thick double layers, however, the difference in relaxation times is accentuated because the charge in the double layer is spread out over a larger spatial region, which does not necessarily charge uniformly. In fact, that $\tau_\rho(r=1)$ is smaller than τ_q for larger values of ϵ (Fig. 13) suggests that regions closer to the surface of the sphere charge faster than regions that are further away.

VII. WEAKLY NONLINEAR RELAXATION FOR THIN DOUBLE LAYERS

A. Dynamical regimes in space-time

For weak applied fields in linear response, the complicated dependence of the Laplace transform solution for large s (short times) above hints at the presence of multiple time

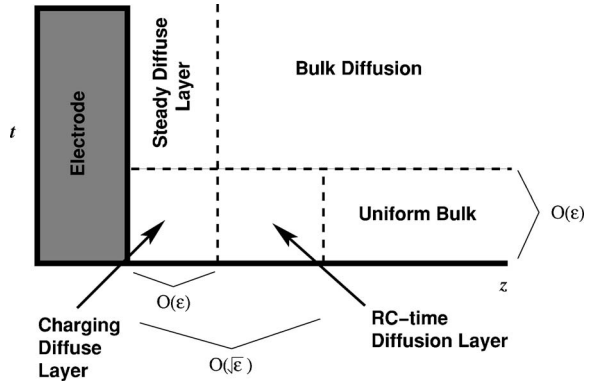

FIG. 14. Five asymptotically distinct regions of space-time that govern the dynamic response of a metal colloid sphere to an applied electric field. Note the nested spatial boundary layers at the *RC* time [$t=O(\epsilon)$].

scales in the charging dynamics. In this section, using boundary-layer methods, we derive asymptotic solutions in the thin double-layer limit ($\epsilon \ll 1$) at somewhat larger electric fields (defined below) for the concentrations and electric potential by solving the leading-order equations at the two dominant time scales (1) the *RC* time $\lambda_D a/D$ and (2) the bulk diffusion time a^2/D. We proceed by seeking the leading-order term (and in some cases, the first-order correction) to the governing equations (19)–(21) with both the spatial *and* the time coordinate scaled to focus on the space-time region of interest.

For the analysis, it is important to realize that the space-time domain is divided into five asymptotically distinct regions (see Fig. 14). At the *RC* time, there exist three spatially significant regions: (i) an $O(\epsilon)$ quasisteady double layer, (ii) an $O(\sqrt{\epsilon})$ dynamically active diffusion layer, and (iii) a quasiequilibrium, uniform bulk electrolyte layer with time-varying harmonic electric potential. At this time scale, the charging dynamics are completely driven by the $O(\sqrt{\epsilon})$ diffusion layer. At the diffusion time, there are only two important spatial regimes: (i) a quasisteady double layer and (ii) a dynamic bulk that evolves through locally electroneutral, diffusion processes.

B. Dynamics at the RC time

1. Uniform bulk and equilibrium double layers

To examine the dynamics at the *RC* time, we rewrite (19)–(21) by rescaling time to the *RC* time using $\tilde{t}=t/\epsilon$:

$$\frac{\partial c}{\partial \tilde{t}} = \epsilon \nabla \cdot (\nabla c + \rho \nabla \phi), \tag{103}$$

$$\frac{\partial \rho}{\partial \tilde{t}} = \epsilon \nabla \cdot (\nabla \rho + c \nabla \phi), \tag{104}$$

$$-\epsilon^2 \nabla^2 \phi = \rho. \tag{105}$$

Since the spatial coordinate is scaled to the bulk length, the leading-order solution of these equations describes the dy-

namics of the bulk during the double-layer charging phase. Substituting a regular asymptotic expansion of the form

$$c(x,t) \sim c_0 + \epsilon c_1 + \epsilon^2 c_2 + \cdots \tag{106}$$

into Eqs. (103)–(105) yields a hierarchy of partial differential equations. By sequentially solving the equations using the initial conditions, it is easy to show that the "outer" solutions at the *RC* charging time scale are

$$c_0(x,t) \equiv 1, \tag{107}$$

$$c_j(x,t) \equiv 0, \quad j = 1,2,3, \ldots, \tag{108}$$

$$\rho_j(x,t) \equiv 0, \quad j = 0,1,2, \ldots, \tag{109}$$

with ϕ_j harmonic at all orders. In other words, the bulk solution can be completely expressed (without a series expansion) as a uniform concentration profile $c(x,t) \equiv 1$ and a time-varying harmonic electric potential ϕ. Note that by taking advantage of spherical geometry and axisymmetry in our problem, we can write the potential as a series in spherical harmonics with zero zonal wave number (i.e., Legendre polynomials in $\cos\theta$):

$$\phi(r,\theta,t) = -E_0 r \cos\theta + \sum_{l=0}^{\infty} P_l(\cos\theta)\frac{A_l(t)}{r^{l+1}} \tag{110}$$

where the radial dependence of each term has been selected so that ϕ automatically satisfies Laplace's equation at all times.

At the *RC* charging time, the $O(\epsilon)$ double layer is in quasiequilibrium, which is easily verified by rescaling the spatial coordinate normal to the particle surface by the dimensionless Debye length ϵ. As mentioned earlier, a quasiequilibrium double layer possesses a structure described by the Gouy-Chapman-Stern model. For convenience, we repeat the GCS solution here:

$$\tilde{c}_{\pm} = \hat{c}e^{\mp\tilde{\psi}}, \quad \tilde{c} = \hat{c}\cosh\tilde{\psi}, \quad \tilde{\rho} = -\hat{c}\sinh\tilde{\psi},$$

$$\tilde{\psi}(z) = 4\tanh^{-1}[\tanh(\zeta/4)e^{-\sqrt{\hat{c}}z}]. \tag{111}$$

Recall that $\tilde{\psi}$ is the excess voltage relative to the bulk, $\tilde{\psi} = \tilde{\phi} - \hat{\phi}$, and that the tilde and caret are used to indicate quantities within and just outside the double layer, respectively. Also, we reiterate that unlike the 1D case, ζ is not a constant but is a function of the spatial position along the electrode surface.

Since the bulk concentration at the *RC* time is uniform, the double-layer structure is given by (111) with $\hat{c}$ set equal to 1. Notice that at the *RC* time, bulk concentration gradients have not yet had time to form, so the variation of the diffuse-layer concentration and charge density along the surface of the sphere is solely due to a nonuniform ζ potential.

2. $O(\sqrt{\epsilon})$ diffusion layer

The analysis in the previous section leads us to an apparent paradox. The dynamics of the system seem to have been lost since both the bulk and the boundary layers are in quasiequilibrium at leading order; neither layer drives its own dynamics. As discussed in [1], the resolution to this paradox lies in the time-dependent flux matching between the bulk and the boundary layer. Unfortunately, it is inconsistent to directly match the bulk to the boundary layer; there must exist a nested $O(\sqrt{\epsilon})$ diffusion layer in order to account for the buildup of both surface charge and surface excess neutral salt concentration.

Mathematically, the presence of the diffusion layer at the *RC* time scale appears as a dominant balance in the transport equations by rescaling the spatial coordinate in the normal direction to the surface by $\sqrt{\epsilon}$ to obtain

$$\frac{\partial\bar{c}}{\partial\tilde{t}} = \epsilon^2\nabla_s\cdot(\nabla_s\bar{c} + \bar{\rho}\nabla_s\bar{\phi}) + \frac{\partial}{\partial z'}\left(\frac{\partial\bar{c}}{\partial z'} + \bar{\rho}\frac{\partial\bar{\phi}}{\partial z'}\right), \tag{112}$$

$$\frac{\partial\bar{\rho}}{\partial\tilde{t}} = \epsilon^2\nabla_s\cdot(\nabla_s\bar{\rho} + \bar{c}\nabla_s\bar{\phi}) + \frac{\partial}{\partial z'}\left(\frac{\partial\bar{\rho}}{\partial z'} + \bar{c}\frac{\partial\bar{\phi}}{\partial z'}\right), \tag{113}$$

$$-\epsilon^2\nabla_s^2\bar{\phi} - \epsilon\frac{\partial^2\bar{\phi}}{\partial z'^2} = \bar{\rho}. \tag{114}$$

Here the overbar denotes the diffusion-layer solution at the *RC* time and $z' = Z/\sqrt{\epsilon}$ is the spatial coordinate in the direction normal to the surface. Notice that at this length scale, the system is not in quasiequilibrium as it is at the bulk and Debye length scales. It is, however, locally electroneutral at leading order as a result of (114).

As the double layer charges, it absorbs an $O(\epsilon)$ amount of charge and neutral salt from the $O(\sqrt{\epsilon})$ diffusion layer. Therefore, we expect concentration changes within the diffusion to be on the order of $\sqrt{\epsilon}$, which motivates the use of an asymptotic expansion of the form

$$\bar{c}(x,t) \sim \bar{c}_0 + \epsilon^{1/2}\bar{c}_{1/2} + \epsilon\bar{c}_1 + \cdots. \tag{115}$$

Using this expansion in (112)–(114), we find that the leading-order equations are

$$\frac{\partial\bar{c}_0}{\partial\tilde{t}} = \frac{\partial^2\bar{c}_0}{\partial z'^2}, \tag{116}$$

$$\frac{\partial}{\partial z'}\left(\bar{c}_0\frac{\partial\bar{\phi}_0}{\partial z'}\right) = 0, \tag{117}$$

$$\bar{\rho}_0 = 0. \tag{118}$$

The initial conditions and boundary condition as $z' \to \infty$ for these equations are $\bar{c}_0(t=0) \equiv 1$ and $\bar{c}_0(z' \to \infty) = 1$, respectively. The boundary condition at $z' = 0$ is given by flux matching with the double layer. Rescaling space and time in (60) and (61), we find that the appropriate flux boundary conditions for the diffusion layer are

$$\frac{\partial q}{\partial\tilde{t}} = \epsilon\nabla_s\cdot(q\nabla_s\ln\bar{c} + w\nabla_s\bar{\phi}) + \frac{1}{\sqrt{\epsilon}}\bar{c}\frac{\partial\bar{\phi}}{\partial z'}, \tag{119}$$

$$\frac{\partial w}{\partial \tilde{t}} = \epsilon \nabla_s \cdot (w \nabla_s \ln \bar{c} + q \nabla_s \bar{\phi}) + \frac{1}{\sqrt{\epsilon}} \frac{\partial \bar{c}}{\partial z'}. \tag{120}$$

Thus, the leading-order flux boundary conditions, which appear at $O(1/\sqrt{\epsilon})$, are

$$\bar{c}_0 \frac{\partial \bar{\phi}_0}{\partial z'} = 0, \tag{121}$$

$$\frac{\partial \bar{c}_0}{\partial z'} = 0. \tag{122}$$

The leading-order solutions in the diffusion layer, $\bar{c}_0 \equiv 1$ and $\bar{\phi}_0 = \phi(Z \to 0)$, are easily determined by applying the initial and boundary conditions to (116)–(118).

To obtain dynamics, we must examine the first-order correction to the solution. At the next higher order, the governing equations are

$$\frac{\partial \bar{c}_{1/2}}{\partial \tilde{t}} = \frac{\partial^2 \bar{c}_{1/2}}{\partial z'^2}, \tag{123}$$

$$\frac{\partial^2 \bar{\phi}_{1/2}}{\partial z'^2} = 0, \tag{124}$$

$$\bar{\rho}_{1/2} = 0, \tag{125}$$

where we have made use of the leading-order solution to simplify (124). Again, the initial conditions and boundary condition at infinity are simple: $\bar{c}_{1/2}(t=0) \equiv 0$ and $\bar{c}_{1/2}(z' \to \infty) = 0$. The flux boundary conditions at $z'=0$, however, are more interesting because they involve the charging of the double layer:

$$\frac{\partial q}{\partial \tilde{t}} = \left. \frac{\partial \bar{\phi}_{1/2}}{\partial z'} \right|_{z=0}, \tag{126}$$

$$\frac{\partial w}{\partial \tilde{t}} = \left. \frac{\partial \bar{c}_{1/2}}{\partial z'} \right|_{z=0}. \tag{127}$$

Thus, simple diffusion of neutral salt at $x = O(\sqrt{\epsilon})$ driven by absorption into the $O(\epsilon)$ double layer dominates the dynamics of the diffusion layer. From (124) and (126), we see that the electric potential possesses a linear profile with slope given by the rate of surface charge buildup in the double layer:

$$\bar{\phi} \sim \phi(Z \to 0) + \epsilon^{1/2} \left(\frac{\partial q}{\partial \tilde{t}} \right) z'. \tag{128}$$

Note that the constant term at $O(\sqrt{\epsilon})$ is forced to be zero by matching with the bulk electric potential since all higher-order corrections to the bulk potential are identically zero.

3. Effective boundary conditions across entire diffusion layer

It is precisely the fact that the electric potential has the form (128) that justifies the common approach of asymptotic matching directly between the bulk and the double layer [1,16,17]. For instance, the time-dependent matching used by Bazant, Thornton, and Ajdari [1] rests on the implicit assumption that the leading-order electric field in the diffusion layer is a constant and appears at $O(\sqrt{\epsilon})$ so that

$$\left. \frac{\partial \phi}{\partial Z} \right|_{Z=0} = \frac{1}{\sqrt{\epsilon}} \left(\frac{\partial \bar{\phi}}{\partial z'} \right) \Bigg|_{z' \to \infty} \sim \left. \frac{\partial \bar{\phi}_{1/2}}{\partial z'} \right|_{z' \to \infty} = \frac{\partial q}{\partial \tilde{t}}. \tag{129}$$

Similarly, the definition of the ζ potential and the Stern boundary condition (30) across the entire diffusion layer require that $\bar{\phi} \sim \phi$ $(Z \to 0)$ at leading order.

4. Leading-order dynamics

Using the results of our discussion, we now derive the leading-order equations that govern the charging dynamics on the surface of the sphere. Since charging is nonuniform over the electrode surface, the equations take the form of partial differential equations on the surface of the sphere. Defining $\Psi(\theta, \phi) \equiv v - \phi(r=1, \theta, \phi)$, we can write the Stern boundary condition (30) and the double-layer charging equation (129) as

$$\zeta + 2\delta \sinh(\zeta/2) = \Psi, \tag{130}$$

$$C(\Psi) \frac{\partial \Psi}{\partial \tilde{t}} = \frac{\partial \phi}{\partial n}, \tag{131}$$

where we have introduced the leading-order differential double-layer capacitance $C(\Psi) = -\partial q / \partial \Psi$ and used the fact that $\hat{c} = 1$ at the RC time. Together with (56), Eqs. (130) and (131) form a complete set of boundary conditions for the leading-order electric potential in the bulk region. To compute the double-layer capacitance, we can combine (56) with (130) to obtain

$$C = \frac{1}{\operatorname{sech}(\zeta/2) + \delta}. \tag{132}$$

Since C depends on $\tilde{\Psi}$ (via ζ), the charging equation (131) is nonlinear, which makes the problem analytically intractable.

For small applied fields (where $\zeta \approx E_0$ is a reasonable approximation), analytical progress can be made by linearizing the double-layer capacitance around $\zeta = 0$ to obtain $C \sim 1/(1+\delta)$. This approximation leads to a linear charging equation making it possible to solve the equations as an expansion in spherical harmonics. Substituting the expansion (110) into (131) and the definition of Ψ, we obtain a decoupled system of ordinary differential equations for the expansion coefficients,

$$\frac{dA_0}{d\tilde{t}} + (1+\delta) A_0 = \frac{dv}{d\tilde{t}},$$

$$\frac{dA_1}{d\tilde{t}} + 2(1+\delta) A_1 = -(1+\delta) E_0 + \frac{dE_0}{d\tilde{t}},$$

$$\frac{dA_l}{d\tilde{t}} + (1+l)(1+\delta)A_l = 0, \quad l > 1. \tag{133}$$

To retain generality, we have allowed for the possibility that the applied electric field and surface potential are time varying. For the case of a steady surface potential and uniform applied field, we find that the bulk electric potential is

$$\phi = \frac{v}{r}e^{-(1+\delta)\tilde{t}} - E_0 r\cos\theta\left(1 + \frac{1}{2r^3}(1-3e^{-2(1+\delta)\tilde{t}})\right) \tag{134}$$

where we have assumed that both the surface potential and the electric field are suddenly switched on at $\tilde{t}=0$. The initial condition in this situation is that of a conducting sphere at potential v in a uniform applied electric field E_0: $\phi = v - E_0 r\cos\theta(1-1/r^3)$.

Using (134), the double-layer potential and total diffuse charge are easily determined to be

$$\Psi = v(1-e^{-(1+\delta)\tilde{t}}) + \frac{3}{2}E_0\cos\theta(1-e^{-2(1+\delta)\tilde{t}}), \tag{135}$$

$$q \sim -\frac{v}{1+\delta}(1-e^{-(1+\delta)\tilde{t}}) - \frac{3}{2(1+\delta)}E_0\cos\theta(1-e^{-2(1+\delta)\tilde{t}}). \tag{136}$$

These results are consistent with the calculations by Bazant and Squires [16,17], which is expected since the low-applied-field limit corresponds to the regime where the total diffuse charge is linearly related to the ζ potential (and therefore the total double-layer potential). It is worth mentioning that in the common situation where the surface potential is set well before $t=0$, then the first term in each of the above three expressions is not present. Analogous double-layer charging formulas for the cylinders are shown in Table IV.

TABLE IV. Formulas for double-layer charging of metallic cylinders and spheres at weak applied electric fields at the *RC* time. In these formulas, the potential v of the particle is set to zero.

	Cylinder[a]	Sphere
ϕ	$-E_0 r\cos\theta\left(1+\frac{1}{r^2}(1-2e^{-(1+\delta)t}\right)$	$-E_0 r\cos\theta\left(1+\frac{1}{2r^3}(1-3e^{-2(1+\delta)t}\right)$
Ψ	$2E_0\cos\theta(1-e^{-(1+\delta)t})$	$\frac{3}{2}E_0\cos\theta(1-e^{-2(1+\delta)t})$
q	$-\frac{2}{1+\delta}E_0\cos\theta(1-e^{-(1+\delta)t})$	$-\frac{3}{2(1+\delta)}E_0\cos\theta(1-e^{-2(1+\delta)t})$

[a] θ measured from vertical axis.

5. Numerical model

For larger applied fields, the nonlinear double-layer capacitance forces us to use numerical solutions to gain physical insight. Since the bulk electric potential is a time-varying harmonic function, it is most natural to numerically model the evolution equation for the potential using a multipole expansion with harmonic terms. Truncating (110) after a finite number of terms yields a discrete solution of the form

$$\hat{\phi}(r,\theta,\tilde{t}) = -E_0 r\cos\theta + \sum_{l=0}^{N}\frac{A_l(\tilde{t})}{r^{l+1}}P_l(\cos\theta) \tag{137}$$

where the unknowns are the time-dependent coefficients in the expansion. By using (137) and enforcing that (131) is satisfied at the collocation points $\theta_i = i\pi/N$, we derive a system of ordinary differential equations (ODEs) for the coefficients $A_l(\tilde{t})$:

$$\mathbf{CP}\frac{d\vec{A}}{d\tilde{t}} = E_0\mathbf{P}(:,2) + \mathbf{Q}\vec{A} \tag{138}$$

where $\vec{A}$ is the vector of expansion coefficients, $\mathbf{P}$ and $\mathbf{Q}$ are collocation matrices that relate the expansion coefficients to ϕ and $\partial\phi/\partial n$, respectively, and $\mathbf{C}$ is a diagonal matrix that represents the double-layer capacitance at the collocation points. Note that $\mathbf{P}(:,2)$ (which represents the second column of $\mathbf{P}$ in MATLAB notation) is the discrete representation of $P_1(\cos\theta)=\cos\theta$, so the term $E_0\mathbf{P}(:,2)$ accounts for the applied background potential. The explicit forms for the collocation matrices and the discrete double-layer capacitance

$$\mathbf{P} = \begin{bmatrix} P_0(\cos\theta_0) & P_1(\cos\theta_0) & \cdots & P_N(\cos\theta_0) \\ P_0(\cos\theta_1) & P_1(\cos\theta_1) & \cdots & P_N(\cos\theta_1) \\ \vdots & \vdots & \ddots & \vdots \\ P_0(\cos\theta_N) & P_1(\cos\theta_N) & \cdots & P_N(\cos\theta_N) \end{bmatrix}, \quad \mathbf{Q} = \begin{bmatrix} P_0(\cos\theta_0) & 2P_1(\cos\theta_0) & \cdots & (N+1)P_N(\cos\theta_0) \\ P_0(\cos\theta_1) & 2P_1(\cos\theta_1) & \cdots & (N+1)P_N(\cos\theta_1) \\ \vdots & \vdots & \ddots & \vdots \\ P_0(\cos\theta_N) & 2P_1(\cos\theta_N) & \cdots & (N+1)P_N(\cos\theta_N) \end{bmatrix},$$

$$\mathbf{C} = \mathrm{diag}(C(\Psi(\theta_0), C(\Psi(\theta_1), \ldots, C(\Psi(\theta_N)). \tag{139}$$

The system of ODEs for the expansion coefficients is easily solved using MATLAB's built-in ODE solvers by multiplying (138) through by $(\mathbf{CP})^{-1}$ and writing a simple function to evaluate the resulting right-hand side function.

6. Dipole-dominated charging

From the numerical solution of the charging equation (131), we see that when the sphere is electrically grounded, charging is dominated by the dipolar contribution to the re-

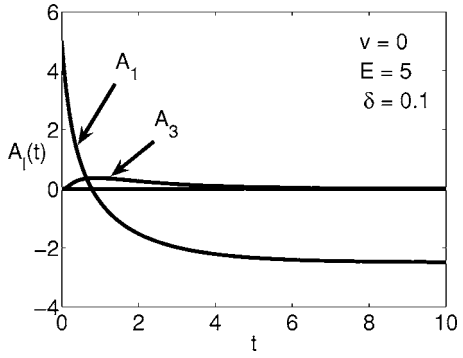

FIG. 15. Time evolution of the dominant coefficients in the Legendre polynomial expansion of the bulk electric potential in the weakly nonlinear regime at the *RC* time. In this figure $v=0$, $E=5$, and $\delta=0.1$. Notice that the dipolar term dominates the solution.

sponse (see Fig. 15). While the nonlinear capacitance does in fact allow higher harmonics to contribute to the response, the higher harmonics only play a small role even at larger applied fields. As expected, when the sphere is kept at zero voltage, the antisymmetry between the upper and lower hemispheres is not broken and only odd terms contribute to the series solution (110). However, as shown in Fig. 16, if a nonzero potential is applied to the sphere, all harmonics contribute to the solution. In this case, the dominant contributions come from the monopolar and dipolar terms.

The dipolar nature of double-layer charging forms the foundation of much of the work on the charging of colloid particles over the past half century. For instance, the nonequilibrium double layer is often characterized in terms of the induced dipole moment [53]. As shown in (134)–(136), the monopole and dipole contributions are the only contributions in a linearized theory. Our numerical investigations demonstrate that, even for the nonlinear theory, the monopole and dipole response dominates the total response. Our results provide additional theoretical support for the focus on the dipole response when studying colloid particles in applied fields.

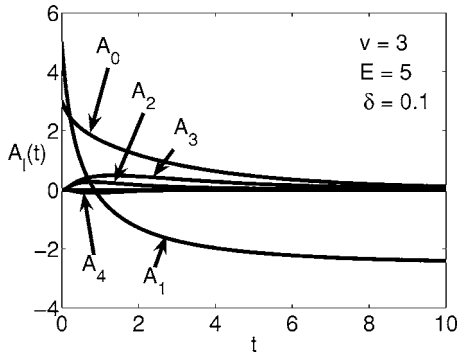

FIG. 16. Time evolution of the dominant coefficients in the Legendre polynomial expansion of the bulk electric potential in the weakly nonlinear regime at the *RC* time when the sphere has a nonzero applied voltage. In this figure $v=3$, $E=5$, and $\delta=0.1$. Note that both symmetric and antisymmetric terms make non-negligible contributions.

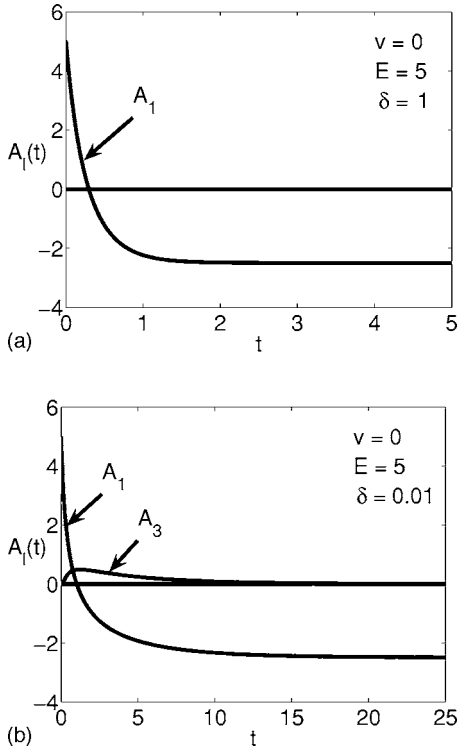

FIG. 17. Time evolution of the dominant coefficients in the Legendre polynomial expansion of the bulk electric potential in the weakly nonlinear regime at the *RC* time for low (top) and high (bottom) Stern capacitance values. In these figures $v=0$ and $E=5$. Note that double-layer charging is retarded when δ is small but that the slowdown in double-layer charging is suppressed for larger δ values.

7. Extended double-layer charging

The slowing of double-layer charging is one important consequence of nonlinearity in the double-layer capacitance (see Fig. 17). However, as shown in Fig. 17 extended charging only occurs for $\delta \ll 1$. Mathematically, we only see slowed charging at small values of δ because the double-layer capacitance (132) can only become as small as $1/\delta$, which occurs at large ζ potentials. For sufficiently small δ, charging is slowed at higher applied fields because the $\mathrm{sech}(\zeta/2)$ term in the denominator of the double-layer capacitance (132) becomes negligible when $\zeta \gg -2\ln(\delta/2)$.

C. Dynamics at the diffusion time scale

In this section, we examine the response of the system at the diffusion time scale. We find that the only dynamic process is diffusion of neutral salt within the bulk in response to surface adsorption that occurred at the *RC* time scale. Since the total amount of neutral salt absorbed by the diffuse charge layers during the charging phase is an $O(\epsilon)$ quantity, the bulk concentration only needs to decrease by $O(\epsilon)$ to compensate. Thus, we find that dynamics are not present at leading order; rather, they appear only in higher-order corrections. Also, at the diffusion time, surface transport, which is negligible at the *RC* time scale, becomes important.

1. Leading-order bulk and double-layer solutions

Substituting an asymptotic series into (19)–(21), we obtain the leading-order bulk equations

$$\frac{\partial c_0}{\partial t} = \nabla^2 c_0, \tag{140}$$

$$\nabla^2 \phi_0 = 0. \tag{141}$$

Applying the initial conditions (obtained by matching to the solution at the RC time) and the leading-order boundary conditions [derived from the effective flux boundary conditions (60) and (61)] yields the simple leading-order solutions for a sphere

$$c_0(\vec{x},t) \equiv 1, \tag{142}$$

$$\phi_0(\vec{x},t) = -E_0 r \cos\theta\left(1 + \frac{1}{2r^3}\right), \tag{143}$$

and a cylinder

$$c_0(\vec{x},t) \equiv 1, \tag{144}$$

$$\phi_0(\vec{x},t) = -E_0 r \cos\theta\left(1 + \frac{1}{r^2}\right). \tag{145}$$

Notice that there is no time dependence for either the concentration or the electric potential. It is worth mentioning that for a general geometry, the initial condition is a uniform concentration profile with the electric potential of an insulator in an applied field and the boundary conditions (which are consistent with the initial conditions) are

$$c_0 \frac{\partial \phi_0}{\partial n} = 0 \quad \text{and} \quad \frac{\partial c_0}{\partial n} = 0. \tag{146}$$

At the diffusion time scale, the double layer continues to remain in quasiequilibrium, so its leading-order structure is given by (111) with the bulk concentration set equal to 1. However, unlike the double layer at the RC time scale, the leading-order ζ potential is not evolving, so the leading-order double-layer structure is static in time.

2. Higher-order bulk diffusion

In order to see dynamics, we need to consider the first-order correction to (140) and (141):

$$\frac{\partial c_1}{\partial t} = \nabla^2 c_1, \tag{147}$$

$$\nabla^2 \phi_1 = -\nabla c_1 \cdot \nabla \phi_0. \tag{148}$$

The boundary conditions for these equations are a bit more complicated. Using (60) and (61) and taking into account the leading-order solutions, we find that the boundary conditions for the $O(\epsilon)$ equations are

$$q_0 \delta^+(t) = \nabla_s \cdot (w_0 \nabla_s \phi_0) - \frac{\partial \phi_1}{\partial n}, \tag{149}$$

$$w_0 \delta^+(t) = \nabla_s \cdot (q_0 \nabla_s \phi_0) - \frac{\partial c_1}{\partial n}, \tag{150}$$

where q_0 and w_0 are the leading-order equilibrium surface charge density and surface excess neutral salt concentration. As mentioned earlier, at the diffusion time scale, these quantities are static in time. Also, note the presence of the δ functions in time, which account for the "instantaneous" adsorption of charge and neutral salt from the bulk during the at the RC time [1].

Mathematically, the appearance of the δ functions is a consequence of the connection between the time derivative of double-layer quantities at the two time scales in the asymptotic limit $\epsilon \to 0$. To illustrate this connection, consider the time derivative of the surface charge density q. Let t and $\tilde{t}$ be scaled to the diffusion and RC times, respectively, so that $t = \epsilon \tilde{t}$. At these two time scales, the surface charge density can be written as $q(t)$ and $\tilde{q}(\tilde{t})$, which are simply related by $q(t) = \tilde{q}(\tilde{t})$. The time derivatives, however, are related by

$$\frac{\partial q}{\partial t}(t) = \frac{1}{\epsilon}\frac{\partial \tilde{q}}{\partial \tilde{t}}(t/\epsilon). \tag{151}$$

Therefore, for nonzero t, $\frac{\partial q}{\partial t} = 0$ in the asymptotic limit because $\frac{\partial \tilde{q}}{\partial \tilde{t}}(t/\epsilon)$ approaches zero faster than linearly as $\epsilon \to 0$ [as an example, see (136)]. In contrast, for $t = 0$, $\frac{\partial q}{\partial t}$ is infinite because $\frac{\partial \tilde{q}}{\partial \tilde{t}}(0)$ has a fixed nonzero value. Next, consider the following integral with $t_2 > 0$:

$$\int_{t_1}^{t_2} \frac{\partial q}{\partial t} dt = \int_{t_1/\epsilon}^{t_2/\epsilon} \frac{\partial \tilde{q}}{\partial \tilde{t}} d\tilde{t} = \tilde{q}(t_2/\epsilon) - \tilde{q}(t_1/\epsilon). \tag{152}$$

In the asymptotic limit, the integral approaches zero for nonzero t_1 but approaches $\tilde{q}(\infty)$ when t_1 equals zero. Putting the above properties together, we see that $\frac{\partial q}{\partial t}(t)$ is indeed a one-sided δ function of strength $\tilde{q}(\infty) = q_0$.

In contrast to one-dimensional systems, the boundary layers play a more active role in the evolution of the bulk concentrations because surface conduction continues to play a role well beyond the initial injection of ions at $t = 0$. Note, however, that the surface conduction terms in (149) and (150) are static, so they essentially impose fixed normal flux boundary conditions on the $O(\epsilon)$ bulk equations.

3. Comparison with the analysis of Dukhin and Shilov

It is interesting to compare and contrast our weakly nonlinear analysis with the work of Dukhin and Shilov [42,45] on the polarization of the double layer for highly charged, spherical particles in weak applied fields. In both cases, bulk concentration variations and diffusion processes appear as a higher-order correction to a uniform background concentration and are driven by surface conduction. However, the significance of the surface conduction term arises for different reasons. As mentioned earlier, the small parameters that control the size of the correction are different in the two analyses. In Dukhin and Shilov's analysis, the small parameters are ϵ and E_0. Because they essentially use asymptotic series in E_0 as the basis for their analysis, they require that the

double layer be highly charged in order for surface conduction to be of the same order of magnitude as the $O(E_0)$ normal flux of ions from the bulk. In other words, because the size of the surface conduction is proportional to E_0, in order for surface conduction to be of the same order of magnitude as the normal flux, the surface charge density must be an $O(1)$ quantity: $\epsilon q = 2\epsilon \sinh(\zeta_0/2) = O(1)$. In contrast, we use asymptotic series in ϵ in our analysis and do not restrict E_0 to be small, so the surface conduction and normal flux of ions from the bulk have the same order of magnitude for small $O(\epsilon)$ surface charge densities regardless of the strength of the applied electric field (as long as it is not so large that the asymptotic analysis breaks down). Thus, our weakly nonlinear analysis complements the work of Dukhin and Shilov by extending their analysis to stronger applied electric fields and the case where the surface charge density is induced by the applied field rather than fixed by surface chemistry of the colloid particle.

VIII. STRONGLY NONLINEAR RELAXATION

A. Definition of "strongly nonlinear"

The weakly nonlinear analysis of the thin double-layer limit in the previous section assumes that the dimensionless surface charge density α and surface salt density β remain uniformly small. For our PNP model, we can estimate when this assumption becomes significantly violated using Eq. (65) with $\zeta = E_0 a/(1+\delta)$ and $C = C_0$, which occurs at fields above a critical value at least a few times the thermal voltage,

$$E_0 > \frac{2kT}{z_+ ea}\left(1 + \frac{\lambda_S}{\lambda_D}\right)\ln\left(\frac{a}{\lambda}\right). \tag{153}$$

As discussed in Sec. IV, this condition also implies that surface adsorption of ions from the bulk is large enough to trigger significant bulk diffusion and surface transport through the double layer, in steady state. However, as noted by Bazant *et al.* [1], weakly nonlinear asymptotics breaks down during relaxation dynamics at somewhat smaller voltages, $\alpha/\sqrt{\pi\epsilon} < 1$, or (with units restored)

$$E_0 > \frac{kT}{z_+ ea}\left(1 + \frac{\lambda_S}{\lambda_D}\right)\ln\left(\frac{\pi a}{\lambda}\right), \tag{154}$$

since large surface adsorption can occur only temporarily at certain positions. (The factor π in this formula comes from a one-dimensional analysis of bulk diffusive relaxation, which does not strictly apply here, but the rough scale should be correct.)

Beyond the weakly nonlinear regime, there are two main effects that occur: (1) transient, local depletion of the leading-order bulk concentration and (2) surface conduction at the leading order. As in the case of a steady applied field, perhaps the greatest impact of $\alpha = O(1)$ is that we must pay attention to factors of the form ϵe^{ζ} or $\epsilon \sinh(\zeta)$, in addition to factors of ϵ, when ordering terms in asymptotic expansions.

In the thin double-layer limit, the boundary layers are still in quasiequilibrium, as long as the bulk concentration does not approach zero, which would typically require Faradaic reactions consuming ions at the conducting surface [57,67]. Since we only consider ideally polarizable conductors, bulk depletion is driven solely by adsorption of ions in the diffuse layer, which is unlikely to exceed diffusion limitation and produce nonequilibrium space charge, although this possibility has been noted [1]. Therefore, we would like to proceed as in the previous sections and treat the bulk as locally electroneutral with effective boundary conditions.

B. Leading-order equations

Unfortunately, the analysis of the leading-order equations derived in this manner does not appear to be as straightforward as the analysis in the weakly nonlinear limit. The main problem is that it seems difficult to derive uniformly valid leading-order effective boundary conditions along the entire surface of the sphere. For this reason, we merely present the *apparent* leading-order equations for the strongly nonlinear regime and leave a thorough analysis for future work.

At the leading order in the bulk, we find the usual equations for a neutral binary electrolyte:

$$\frac{\partial c_0}{\partial t} = \nabla^2 c_0, \tag{155}$$

$$0 = \boldsymbol{\nabla} \cdot (c_0 \boldsymbol{\nabla} \phi_0) \tag{156}$$

with $\rho = O(\epsilon^2)$. The structure of the boundary layers is described by GCS theory with the concentration and charge density profiles given by (111). Effective boundary conditions for (155) and (156) are derived in the same manner as for a steady applied field except that unsteady terms are retained. Recalling that q and w grow exponentially with the ζ potential, we find that both the surface conduction terms and the time derivatives of the total diffuse charge and excess concentration appear in the leading-order boundary conditions:

$$\epsilon \frac{\partial \tilde{q}_0}{\partial t} = \epsilon \boldsymbol{\nabla}_s \cdot (\tilde{w}_0 \boldsymbol{\nabla}_s \phi_0) - c_0 \frac{\partial \phi_0}{\partial n}, \tag{157}$$

$$\epsilon \frac{\partial \tilde{w}_0}{\partial t} = \epsilon \boldsymbol{\nabla}_s \cdot (\tilde{q}_0 \boldsymbol{\nabla}_s \phi_0) - \frac{\partial c_0}{\partial n}. \tag{158}$$

C. Challenges with strongly nonlinear analysis

It is important to realize that these equations are mathematically much more complicated than the analogous equations in the weakly nonlinear regime. First, the nonlinearity due to the electromigration term explicitly appears in the bulk equations at leading order; the nonlinearity is not removed by the asymptotic analysis. Furthermore, the diffuse-layer concentrations depend on time explicitly through the bulk concentration at the surface in addition to the ζ potential:

$$\tilde{c}_{\pm}(t) = c_{\pm}(t) e^{\mp \tilde{\psi}(t)}. \tag{159}$$

Already, these features of the equations greatly increases the challenge in analyzing the response of the system.

However, the greatest complication to the mathematical model in the strongly nonlinear regime is that the effective boundary conditions (157) and (158) are not uniformly valid over the surface of the sphere (or cylinder). Near the poles, the double layer charges quickly, so the time-dependent and surface transport terms in the effective boundary conditions become $O(1)$ at very short times. In contrast, the amount of surface charge in the double layer near the equator is always a small quantity. Thus, it would seem that near the equator, the only significant terms in the effective boundary conditions are the normal flux terms. Together, these observations suggest that the appropriate set of boundary conditions to impose on the governing equations (155) and (156) depends on the position on the surface of the sphere. Moreover, the position where the boundary conditions switch from one set to the other depends on time as double-layer charging progresses from the pole toward the equator.

IX. CONCLUSION

A. Predictions of the PNP model

In this paper, we have analyzed electrochemical relaxation around ideally polarizable conducting spheres and cylinders in response to suddenly applied background electric fields, using the standard mathematical model of the Poisson-Nernst-Planck equations. Unlike most (if not all) prior theoretical studies, we have focused on the nonlinear response to "large" electric fields, which transfer more than a thermal voltage to the double layer after charging. We have effectively extended the recent nonlinear analysis of Bazant, Thornton, and Ajdari [1] for the one-dimensional charging of parallel-plate blocking electrodes to some other situations in higher dimensions, where the potential of the conductor is not controlled. Instead, electrochemical relaxation in our model problems is driven by a time-dependent background electric field applied around the conductor, whose charges are completely free to relax. We are not aware of any prior analysis of nonlinear response in such problems (whether or not using the PNP equations), and yet it is important in many applications, in microfluidics, colloids, and electrochemical systems, where applied fields or voltages are often well beyond the linear regime.

We have focused on the structure and dynamics of the double layer and the development of bulk concentration gradients. A major goal has been to move beyond the traditional circuit models commonly used to study the linear response of electrochemical systems. Through a combination of analytical and numerical results, we have shown that significantly enhanced ion concentration within the double layer is a generic feature of nonlinear electrochemical relaxation around a conductor. By interacting with the bulk electric field, the enhanced concentration within the double layer leads to large surface current densities. In addition, because the double layer does not charge uniformly over the surface, tangential concentration gradients within the double layer itself lead to surface diffusion. Due to their coupling to bulk transport processes via normal fluxes of ions into the double layer, these surface transport processes drive the formation of bulk concentration gradients.

We have also found that bulk concentration gradients are always present to some degree and play an important role in allowing the system to relax to the steady state. For weak applied fields, they are often neglected because they only appear as a first-order correction to a uniform background concentration profile. However, for strong applied fields, the variations in the bulk concentration become as large as the background concentration, so they cannot be ignored. These bulk concentration gradients lead to bulk diffusion currents which result in net circulation of neutral salt in the region near the metal colloid particle.

Another key contribution of this work is a careful mathematical derivation of general effective boundary conditions for the bulk transport equations in the thin double-layer limit by applying matched asymptotic expansions to the PNP equations. We derive a set of boundary equations that relate the time evolution of excess surface (double-layer) concentrations to surface transport processes and normal flux from the bulk. An interesting feature of the effective boundary conditions is that they explicitly involve the small parameter ϵ and may have different leading-order forms depending on the characteristic time scale and the magnitude of double-layer ion concentrations.

It is beyond the scope of this paper, but worth pursuing, to study strongly nonlinear dynamics in detail, where (according to the PNP equations) the double layer adsorbs enough ions to significantly perturb the bulk concentration and cause surface transport to bulk transport of ions. The challenging issues discussed at the end of Sec. VIII need to be addressed in order to gain a deeper understanding of the rich behavior of metal colloid systems in this practically relevant regime. Also, it would be beneficial to validate solutions of the effective bulk and boundary conditions in the thin double-layer limit against solutions for the full PNP equations. The utility of the thin double-layer approximation cannot be fully appreciated until this comparison is completed.

B. The need for better continuum models

Unfortunately (or fortunately, depending on one's perspective), the theoretical challenge of strongly nonlinear electrochemical relaxation is much deeper than just solving the PNP equations in a difficult regime: It is clear that the dynamical equations themselves must be modified to better describe the condensation of ions in highly charged double layers. As emphasized by Newman [38], the PNP equations are only justified for dilute solutions, since each ion moves in response to an independent stochastic force with constant diffusivity and mobility, interacting with other ions only through the mean long-range Coulomb force. Important effects in concentrated solutions, such as short-range forces, many-body correlations, steric constraints, solvent chemistry, and nonlinear mobility, diffusivity, or permittivity, are all neglected.

It is tempting to trust the PNP equations in the case of a dilute bulk electrolyte around an initially uncharged surface. However, as we have shown, the model predicts its own demise when a large electric field is applied, due to enormous increases in surface concentration in the diffuse part of

the double layer, even if the bulk concentration is small. Note that the condition for strongly nonlinear relaxation (153) or (154) is similar to the condition for the breakdown of the PNP equations—both require applied voltages across the double layer only several times the thermal voltage. In particular, the Gouy-Chapman solution to the PNP equations predicts an absurd concentration of counterions of one per $Å^3$ at the surface for a surprisingly small ζ potential around $5kT/z_+e \approx 0.2$ V even in a fairly dilute $0.01M$ electrolyte. This critical voltage is routinely applied to the double layer in electrochemical systems.

Of course, electrochemists are well aware of this problem; in fact, Stern originally proposed the compact layer of adsorbed ions, outside the continuum region, as a way to cut off the unbounded double-layer capacitance [68]. Since then, various empirical models of the compact layer have appeared [35,36], but steric effects (or other nonlinearities) in concentrated solutions have received much less attention. Borukhov, Andelman, and Orland recently postulated a continuum free energy for ions, taking into account steric repulsion with the usual mean-field electrostatics and minimized it to derive a modified Poisson-Boltzmann equation for the potential in the double layer [69]. Their model predicts a steady, equilibrium profile of ions with a condensed layer at the steric limit for large ζ potentials. By extending this approach to obtain the chemical potential, Kilic, Bazant, and Ajdari [49] have derived modified PNP equations and studied steric effects on double-layer charging, but further model development is still needed, not only for steric effects, but also for field-dependent permittivity and/or diffusivity. The validity of a continuum model at the scale of several atoms in the most condensed part of the double layer must also be viewed with some skepticism.

Nevertheless, in spite of these concerns, it is a natural first step to study nonlinear electrochemical relaxation using the standard PNP equations as we have done. The details of our results will surely change with modified transport equations and/or surface boundary conditions, but we expect some key features to be robust. For example, steric effects could decrease the capacitance of the double layer at large ζ potentials, but surface conduction and adsorption, coupled to bulk diffusion, should still occur, albeit perhaps with smaller magnitude for a given applied field. Also the mathematical aspects of our boundary-layer analysis, such as the derivation of the surface conservation law (49), could be applied to any continuum transport equations.

ACKNOWLEDGMENTS

This work was supported in part by the Office of Science and National Nuclear Security Administration in the Department of Energy under Contract No. DE-FG02-97ER25308 (K.T.C.) and by the MRSEC Program of the National Science Foundation under Grant No. DMR 02-13282 (M.Z.B. and K.T.C.). The authors thank A. Ajdari, J. Choi, and L. H. Oleson for many helpful discussions. We are particularly grateful to L. H. Olesen for pointing out an important term that we had missed in deriving Eq. (47).

[1] M. Z. Bazant, K. Thornton, and A. Ajdari, Phys. Rev. E **70**, 021506 (2004).
[2] M. Sluyters-Rehbach and J. H. Sluyters, *Electroanalytical Chemistry* (Marcel Dekker, New York, 1970), Vol. 4, pp. 1–128.
[3] J. R. Macdonald, Electrochim. Acta **35**, 1483 (1990).
[4] R. Parsons, Chem. Rev. (Washington, D.C.) **90**, 813 (1990).
[5] L. A. Geddes, Ann. Biomed. Eng. **25**, 1 (1997).
[6] T. M. Squires and S. R. Quake, Rev. Mod. Phys. **77**, 977 (2005).
[7] A. Ramos, H. Morgan, N. G. Green, and A. Castellanos, J. Colloid Interface Sci. **217**, 420 (1999).
[8] A. Ajdari, Phys. Rev. E **61**, R45 (2000).
[9] A. González, A. Ramos, N. G. Green, A. Castellanos, and H. Morgan, Phys. Rev. E **61**, 4019 (2000).
[10] N. G. Green, A. Ramos, A. González, H. Morgan, and A. Castellanos, Phys. Rev. E **66**, 026305 (2002).
[11] N. G. Green, A. Ramos, A. González, H. Morgan, and A. Castellanos, Phys. Rev. E **61**, 4011 (2000).
[12] A. Ramos, A. González, A. Castellanos, N. G. Green, and H. Morgan, Phys. Rev. E **67**, 056302 (2003).
[13] V. Studer, A. Pépin, Y. Chen, and A. Ajdari, Microelectron. Eng. **61**, 915 (2002).
[14] V. Studer, A. Pépin, Y. Chen, and A. Ajdari, Analyst (Cambridge, U.K.) **129**, 944 (2004).
[15] F. Nadal, F. Argoul, P. Kestener, B. Pouligny, C. Ybert, and A. Ajdari, Eur. Phys. J. E **9**, 387 (2002).
[16] M. Z. Bazant and T. M. Squires, Phys. Rev. Lett. **92**, 066101 (2004).
[17] T. M. Squires and M. Z. Bazant, J. Fluid Mech. **509**, 217 (2004).
[18] J. A. Levitan, S. Devasenathipathy, V. Studer, Y. Ben, T. Thorsen, T. M. Squires, and M. Z. Bazant, Colloids Surf., A **267**, 122 (2005).
[19] M. Trau, D. A. Saville, and I. A. Aksay, Langmuir **13**, 6375 (1997).
[20] S. Yeh, M. Seul, and B. Shraiman, Nature (London) **386**, 57 (1997).
[21] C. Faure, N. Decoster, and F. Argoul, Eur. Phys. J. B **5**, 87 (1998).
[22] N. G. Green, A. Ramos, and H. Morgan, J. Phys. D **33**, 632 (2000).
[23] C. Marquet, A. Buguin, L. Talini, and P. Silberzan, Phys. Rev. Lett. **88**, 168301 (2002).
[24] F. Nadal, F. Argoul, P. Hanusse, B. Pouligny, and A. Ajdari, Phys. Rev. E **65**, 061409 (2002).
[25] W. D. Ristenpart, I. A. Aksay, and D. A. Saville, Phys. Rev. Lett. **90**, 128303 (2003).
[26] V. A. Murtsovkin, Colloid J. **58**, 341 (1996).
[27] E. Yariv, Phys. Fluids **17**, 051702 (2005).
[28] T. M. Squires and M. Z. Bazant, J. Fluid Mech. (to be published).

[29] K. A. Rose, G. Dougherty, and J. G. Santiago, in *Proceedings of the Ninth International Conference on Miniaturized Systems for Chemistry and Life Sciences*, 2005 (unpublished).
[30] K. A. Rose, J. Meier, G. Dougherty, and J. G. Santiago (unpublished).
[31] D. Saintillan, E. Darve, and E. Shaqfeh, J. Fluid Mech. (to be published).
[32] W. Helfrich, Z. Naturforsch. C **29**, 182 (1974).
[33] M. D. Mitov, P. Méleard, M. Winterhalter, M. I. Angelova, and P. Bothorel, Phys. Rev. E **48**, 628 (1993).
[34] R. Pethig, Crit. Rev. Biotechnol. **16**, 331 (1996).
[35] P. Delahay, *Double Layer and Electrode Kinetics* (Interscience, New York, 1965).
[36] J. O. Bockris and A. K. N. Reddy, *Modern Electrochemistry* (Plenum, New York, 1970).
[37] A. J. Bard and L. R. Faulkner, *Electrochemical Methods* (John Wiley & Sons, New York, 2001).
[38] J. Newman, *Electrochemical Systems*, 2nd ed. (Prentice-Hall, Englewood Cliffs, 1991).
[39] R. J. Hunter, *Foundations of Colloid Science* (Oxford University Press, Oxford, 2001).
[40] J. Lyklema, *Fundamentals of Interface and Colloid Science. Volume II: Solid-Liquid Interfaces* (Academic Press, San Diego, CA, 1995).
[41] I. N. Simonov and V. N. Shilov, Colloid J. USSR **39**, 775 (1977).
[42] S. S. Dukhin and V. N. Shilov, Colloid J. USSR **31**, 564 (1969).
[43] E. J. Hinch and J. D. Sherwood, J. Fluid Mech. **132**, 337 (1983).
[44] E. J. Hinch, J. D. Sherwood, W. C. Chew, and P. N. Sen, J. Chem. Soc., Faraday Trans. 2 **80**, 535 (1984).
[45] V. N. Shilov and S. S. Dukhin, Colloid J. USSR **32**, 90 (1970).
[46] J. J. Bikerman, Trans. Faraday Soc. **36**, 154 (1940).
[47] B. V. Deryagin and S. S. Dukhin, Colloid J. USSR **31**, 277 (1969).
[48] K. T. Chu and M. Z. Bazant (unpublished).
[49] M. S. Kilic, M. Z. Bazant, and A. Ajdari (unpublished).
[50] J. Lyklema, Phys. Rev. E **71**, 032501 (2005).
[51] J. Lyklema, *Fundamentals of Interface and Colloid Science. Volume I: Fundamentals* (Academic Press, San Diego, CA, 1991).
[52] J. D. Ferry, J. Chem. Phys. **16**, 737 (1948).
[53] S. S. Dukhin, Adv. Colloid Interface Sci. **44**, 1 (1993).
[54] S. S. Dukhin and V. N. Shilov, Adv. Colloid Interface Sci. **13**, 153 (1980).
[55] A. A. Kornyshev and M. A. Vorotyntsev, Electrochim. Acta **26**, 303 (1981).
[56] J. R. Macdonald, Trans. Faraday Soc. **16**, 934 (1970).
[57] M. Z. Bazant, K. T. Chu, and B. J. Bayly, SIAM J. Appl. Math. **65**, 1463 (2005).
[58] A. Bonnefont, F. Argoul, and M. Bazant, J. Electroanal. Chem. **500**, 52 (2001).
[59] K. T. Chu, Ph.D. thesis, Department of Mathematics, Massachusetts Institute of Technology, 2005 (unpublished).
[60] J. J. Bikerman, Z. Phys. Chem. Abt. A **163**, 378 (1933).
[61] J. J. Bikerman, Kolloid-Z. **72**, 100 (1935).
[62] L. N. Trefethen, *Spectral Methods in MATLAB* (SIAM, Philadelphia, 2000).
[63] J. P. Boyd, *Chebyshev and Fourier Spectral Methods*, 2nd ed. (Dover Publications, Mineola, NY, 2001).
[64] B. Fornberg, *A Practical Guide to Pseudospectral Methods* (Cambridge University Press, New York, 1998).
[65] P. Debye and H. Falkenhagen, Phys. Z. **29**, 121 (1928).
[66] E. W. Weisstein, MathWorld—A Wolfram Web Resource, http://mathworld.wolfram.com/ModifiedSphericalBesselFunctionoftheSecondKind.html
[67] K. T. Chu and M. Z. Bazant, SIAM J. Appl. Math. **65**, 1485 (2005).
[68] O. Stern, Z. Elektrochem. Angew. Phys. Chem. **30**, 508 (1924).
[69] I. Borukhov, D. Andelman, and H. Orland, Phys. Rev. Lett. **79**, 435 (1997).